Net greenhouse gas balance of fibre wood plantation on peat in Indonesia

Chandra S Deshmukh, Ari P Susanto, Nardi Nardi, Nurholis Nurholis, Sofyan Kurnianto, Yogi Suardiwerianto, M Hendrizal, Ade Rhinaldy, Reyzaldi E Mahfiz, Ankur R Desai, et al.

Article

Net greenhouse gas balance of fibre wood plantation on peat in Indonesia

https://doi.org/10.1038/s41586-023-05860-9

Received: 30 August 2022

Accepted: 16 February 2023

Published online: 5 April 2023

Open access

Check for updates

Chandra S. Deshmukh[1]✉, Ari P. Susanto[1], Nardi Nardi[1], Nurholis Nurholis[1], Sofyan Kurnianto[1], Yogi Suardiwerianto[1], M. Hendrizal[1], Ade Rhinaldy[1], Reyzaldi E. Mahfiz[1], Ankur R. Desai[2], Susan E. Page[3], Alexander R. Cobb[4], Takashi Hirano[5], Frédéric Guérin[6], Dominique Serça[7], Yves T. Prairie[8], Fahmuddin Agus[9], Dwi Astiani[10], Supiandi Sabiham[11] & Chris D. Evans[12]

Tropical peatlands cycle and store large amounts of carbon in their soil and biomass[1–5]. Climate and land-use change alters greenhouse gas (GHG) fluxes of tropical peatlands, but the magnitude of these changes remains highly uncertain[6–19]. Here we measure net ecosystem exchanges of carbon dioxide, methane and soil nitrous oxide fluxes between October 2016 and May 2022 from *Acacia crassicarpa* plantation, degraded forest and intact forest within the same peat landscape, representing land-cover-change trajectories in Sumatra, Indonesia. This allows us to present a full plantation rotation GHG flux balance in a fibre wood plantation on peatland. We find that the *Acacia* plantation has lower GHG emissions than the degraded site with a similar average groundwater level (GWL), despite more intensive land use. The GHG emissions from the *Acacia* plantation over a full plantation rotation (35.2 ± 4.7 tCO_2-eq ha^{-1} $year^{-1}$, average ± standard deviation) were around two times higher than those from the intact forest (20.3 ± 3.7 tCO_2-eq ha^{-1} $year^{-1}$), but only half of the current Intergovernmental Panel on Climate Change (IPCC) Tier 1 emission factor (EF)[20] for this land use. Our results can help to reduce the uncertainty in GHG emissions estimates, provide an estimate of the impact of land-use change on tropical peat and develop science-based peatland management practices as nature-based climate solutions.

Over the Holocene, tropical peatlands have accumulated at least 75 Gt of carbon (C) in partially decomposed debris (wood, roots, litter, leaves) under waterlogged anoxic environments[1–5]. A fine balance between hydrology, ecology and landscape morphology has resulted in this long-term C store[6–8]. Climate and other environmental changes are, however, affecting this C store as a result of warming, drying conditions and change in disturbance rates[9–17]. Particularly, decreased rainfall, increased seasonality and frequent days without rainfall are resulting in GWL drawdowns[7,12,13], which cause C loss[14–17].

Tropical peatlands are among the world's most threatened ecosystems owing to land demand driven by population growth and economic development[21]. In Southeast Asia, which hosts at least one-third of the total tropical peatlands[3,4], most peatland conversion has occurred since the late 1990s[21]. A total peatland area of 7.8 million hectares is managed for agriculture and silviculture, of which more than one million hectares are under fibre wood (mostly *A. crassicarpa*) plantations[21]. Artificial GWL drawdown in agriculture and plantations on peatland exposes previously accumulated peat organic material to oxygen and promotes aerobic decomposition of organic C, resulting in carbon dioxide (CO_2) emissions[22,23] and associated land subsidence[24–26]. At present, the IPCC Tier 1 CO_2 EF[20] for short-rotation tree plantations on tropical peat is entirely based on the use of short-term measurements from the 3–8 years after drainage using subsidence[22] and soil-chamber[23] techniques. Furthermore, tropical peatlands emit methane (CH_4)[27,28] and nitrous oxide (N_2O)[17,29], potent GHGs, yet assessments of the contributions made by these gases to the full peatland GHG balance are scarce[20]. Existing estimates of GHG emissions from tropical peatlands continue to be debated[20,30] with large observed variability (0.04–2.79 $GtCO_2$-eq $year^{-1}$)[18] and resulting uncertainty[19].

From a climate-forcing perspective, the effects of a land-use change on the atmospheric GHG concentrations (that is, the extra GHG fluxes that the atmosphere will see because of current land use) will be determined by the change in emissions relative to those occurring before the land-use change[17,31]. Despite the increasing awareness of the significance of GHG fluxes from managed peatlands, there have been few experimental studies evaluating the GHG balance before and after a land-use change has occurred. Thus, a better quantitative and process-based knowledge of how the tropical peat C store responds to land-use change under current climate conditions is an urgent area of enquiry that can inform strategies for responsible peatland management[32] under national and global frameworks of climate change.

[1]Asia Pacific Resources International Ltd., Pelalawan Regency, Indonesia. [2]Department of Atmospheric and Oceanic Sciences, University of Wisconsin-Madison, Madison, WI, USA. [3]School of Geography, Geology and the Environment, University of Leicester, Leicester, UK. [4]Singapore-MIT Alliance for Research and Technology, Singapore, Singapore. [5]Research Faculty of Agriculture, Hokkaido University, Sapporo, Japan. [6]Géosciences Environnement Toulouse, CNRS, IRD, Université Paul-Sabatier, Toulouse, France. [7]LAERO, Université de Toulouse, CNRS, IRD, UT3, Toulouse, France. [8]UNESCO Chair in Global Environmental Change, Université du Québec à Montréal, Montréal, Québec, Canada. [9]National Research and Innovation Agency (BRIN), Cibinong, Indonesia. [10]Faculty of Forestry, Tanjungpura University, Pontianak, Indonesia. [11]Department of Soil Science and Land Resources, IPB University, Bogor, Indonesia. [12]UK Centre for Ecology & Hydrology, Bangor, UK. ✉e-mail: chandra_deshmukh@aprilasia.com

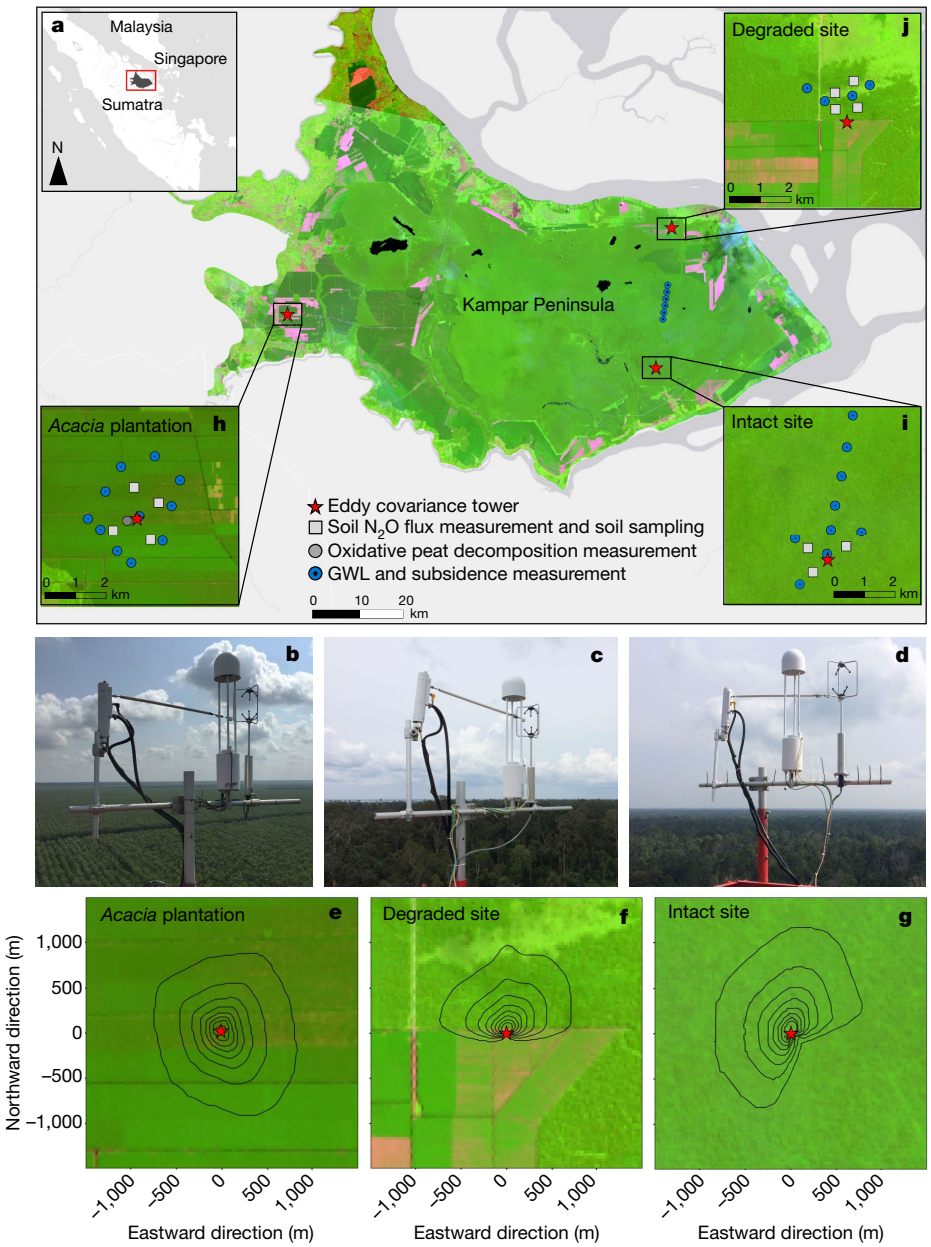

Fig. 1 | Location of the study area, Kampar Peninsula in Sumatra, Indonesia. **a**, Location of research sites with satellite images from Landsat 8 (source: https://earthexplorer.usgs.gov/). Photographs of the eddy covariance instruments installed at the top of the tower at *Acacia* plantation (**b**), degraded site (**c**) and intact site (**d**). For detailed site information, see Methods. Integrated eddy covariance footprint contour lines from 10% to 80% in 10% intervals over *Acacia* plantation for October 2016–May 2021 (**e**), degraded site for October 2016–May 2022 (**f**) and intact site for June 2017–May 2022 (**g**). GWL, peat subsidence, oxidative peat decomposition, soil N_2O flux and soil-sampling locations at *Acacia* plantation (**h**), intact site (**i**) and degraded site (**j**). An integrated climatologic footprint analysis indicated that approximately 80% of fluxes originated within 1,000 m in the upwind direction of each tower. Esri, HERE, Garmin, (c) OpenStreetMap contributors and the GIS user community.

This study represents, to the best of our knowledge, the first GHG balance investigation undertaken in any fibre wood plantation on peatland (and indeed any soil type) globally to cover a full plantation rotation and all major GHG flux terms, including biomass C loss owing to plantation establishment, C export in harvested wood and fluvial C exports. We compare the GHG balance at the *Acacia* plantation with more than 5 years of measurements at the degraded site and 5 years of measurements at the intact site (Figs. 1 and 2 and Extended Data Table 1).

CO_2 flux

Over a 4.7-year period encompassing one full *Acacia* plantation rotation (the fourth rotation during 17–22 years after drainage), the average GWL was −0.65 ± 0.17 m, for which a negative GWL indicates that the water level was below the peat surface (Extended Data Table 2). Net ecosystem exchanges of CO_2 (NEE-CO_2; net gaseous CO_2 exchange between ecosystem and atmosphere) varied with plantation age; it was highest (48.4 ± 4.7 tCO_2 ha^{-1} $year^{-1}$) in the first year after planting, lowest (−8.8 ± 4.5 tCO_2 ha^{-1} $year^{-1}$) in the third year with highest tree growth and then rose again to 11.7 ± 6.0 tCO_2 ha^{-1} $year^{-1}$ before harvesting (Extended Data Fig. 1 and Extended Data Table 3) (for which positive NEE-CO_2 values indicate net CO_2 emissions and negative values indicate net CO_2 uptake). The substantial net CO_2 emissions during the early stage of the plantation were mainly because of the low photosynthetic rates of the young trees and also potentially driven by the decomposition of organic matter from harvested residues (that is, leaves, branches,

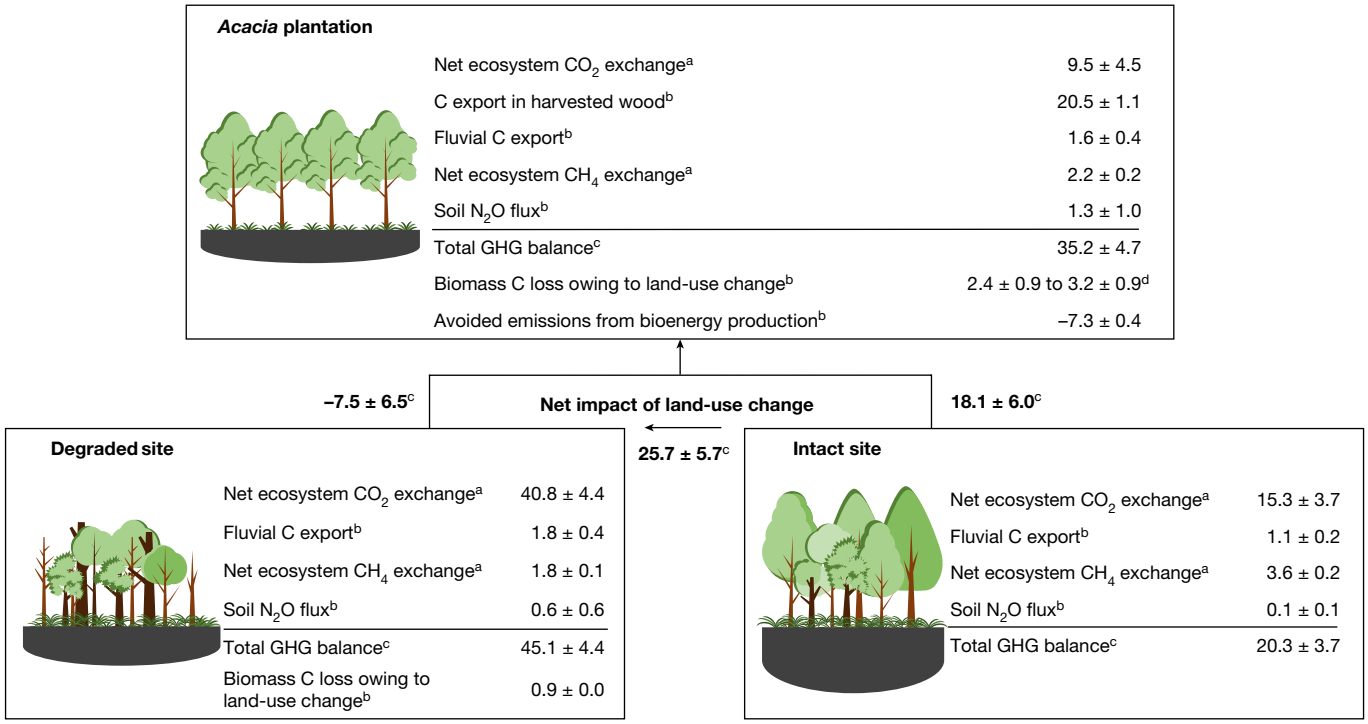

All values are in tCO_2-eq ha^{-1} $year^{-1}$
[a]Values represent average with total uncertainty from random error, friction velocity threshold and gap-filling approach
[b]Values represent average with standard deviation
[c]Values represent total with standard deviation calculated from propagation of errors
[d]Lower and upper ranges represent biomass C loss owing to establishment of *Acacia* plantation from degraded and intact sites, respectively.

Fig. 2 | GHG balance of *Acacia* plantation, degraded and intact peat swamp forest in Sumatra, Indonesia. To quantify total GHG balance in carbon dioxide equivalent (CO_2-eq), we used a sustained-flux global-warming potential (SGWP) of 1, 45 and 270 for CO_2, CH_4 and N_2O, respectively, over a 100-year time period[39]. Total GHG balance = (net ecosystem CO_2 exchange + net ecosystem CH_4-C exchange + fluvial C export + C export in harvested wood, where applicable) + (net ecosystem CH_4 exchange × SGWP) + (soil N_2O flux × SGWP). We assumed that all fluvial C export is ultimately converted to CO_2 (ref. 38). Avoided emissions from bioenergy production are calculated by assuming that 54% of harvested wood is used for bioenergy production (details in Supplementary Methods). The bold numbers indicate net impact of land-use change. Positive values indicate emission to the atmosphere and negative values indicate avoided emission.

bark, roots and stumps) from the previous plantation rotation. After canopy closure, the emissions from oxidative peat decomposition (Extended Data Table 3) were largely outbalanced by high rates of photosynthesis and C fixation (Extended Data Fig. 1). Over the plantation rotation, the average NEE-CO_2 was 9.5 ± 4.5 tCO_2 ha^{-1} $year^{-1}$ (Fig. 2 and Extended Data Table 4). The average peat subsidence rate was −3.0 ± 0.9 cm $year^{-1}$ (Extended Data Table 5) (negative peat subsidence indicates that the ground surface elevation was falling). The C export in harvested wood was 26.3 ± 1.4 tC ha^{-1}, corresponding to 96.5 ± 5.2 tCO_2 ha^{-1} (20.5 ± 1.1 tCO_2 ha^{-1} $year^{-1}$ when annualized over the plantation rotation; Fig. 2 and Extended Data Table 4). Thus, the sum of NEE-CO_2 and C export in harvested wood indicates that the *Acacia* plantation functioned as a CO_2 source of 30.0 ± 4.6 tCO_2 ha^{-1} $year^{-1}$ over the plantation rotation (Fig. 2 and Extended Data Table 4). The observed net CO_2 emissions can be attributed to peat aeration owing to a consistently deep GWL, which enhances heterotrophic respiration rates, combined with a higher soil temperature (intact site = 27.5 ± 0.5 °C versus *Acacia* site = 29.3 ± 1.0 °C; Extended Data Table 2) owing to both canopy-cover loss and GWL drawdown, which further boosts microbial activities and heterotrophic respiration. Note that this calculation conservatively assumed that all harvested C would be returned to the atmosphere as CO_2, as harvested wood was used to produce bioenergy and pulp products, which is common practice for these types of forest plantation.

We also calculated avoided emissions of 7.3 ± 0.4 tCO_2-eq ha^{-1} $year^{-1}$, resulting from the use of tree biomass for bioenergy (see Supplementary Methods), in place of coal burning that would otherwise have been used to support pulp mill operations (Fig. 2 and Extended Data Table 4). This avoided emission through bioenergy production as a by-product of the pulp manufacturing process could be considered to partly offset emissions from the plantation itself, although it clearly does not negate the peat CO_2 emission.

In degraded peat swamp forest, the GWL was consistently low throughout the study period at the degraded site, with an average of −0.69 ± 0.18 m (Extended Data Table 2). NEE-CO_2 did not show clear seasonal and interannual variability. The degraded site emitted 40.8 ± 4.4 tCO_2 ha^{-1} $year^{-1}$ and subsided −3.6 ± 1.2 cm $year^{-1}$ (Fig. 2 and Extended Data Table 3), consistent with previous observations in ref. 17. The observed large CO_2 emissions can be attributed to peat aeration owing to a consistently deep GWL as described for the *Acacia* site. Coarse woody debris from fallen dead trees may also have contributed to the CO_2 emissions, as fallen trees do not decompose instantaneously, providing a lagged but sustained contribution to CO_2 emissions.

In intact peat swamp forest, the GWL followed the seasonal and interannual variability in rainfall (Extended Data Table 2), in line with the initial measurements in ref. 17. The GWL remained below the peat surface for >80% of the study period, indicating that a substantial part of the upper peat profile was aerated. NEE-CO_2 showed strong seasonal and interannual patterns corresponding to the GWL fluctuation (Extended Data Fig. 1). The results indicate that large net CO_2 emissions during dry seasons were not entirely balanced by relatively

small net CO_2 uptake during the wet seasons (Extended Data Fig. 1). Over a 5-year measurement period, the annual NEE-CO_2 ranged from 9.1 ± 3.7 to 25.6 ± 4.1 tCO_2 ha^{-1} $year^{-1}$, with an average value of 15.3 ± 3.7 tCO_2 ha^{-1} $year^{-1}$ (Extended Data Table 3). The CO_2 emissions owing to GWL drawdown are consistent with previous studies in tropical peatlands in which reduced peat accumulation rates[8,15], a hiatus in peat genesis[33] or even C loss[14–17] have been reported in response to droughts driven by intense and frequent El Niño–Southern Oscillation activity.

The evapotranspiration measurements clearly indicate that actual daily evapotranspiration (4.2 mm day^{-1}) exceeded daily rainfall for around 76% of the study period (Extended Data Table 2). Notably, we observed more than 220 days without rainfall every year (Extended Data Table 2). During days without rainfall, the GWL would recede at an average rate of 10.3 mm day^{-1}, resulting from the seepage and evapotranspiration in this ombrotrophic environment. The seepage rates owing to groundwater and subsurface flows, as calculated from GWL drawdown between midnight and 06:00 local time (when evapotranspiration is negligible; Extended Data Fig. 2), was 1.4 mm during a single 12-h night (that is, 2.8 mm day^{-1}), which is similar to a pristine tropical peatland in Brunei[7]. The evapotranspiration resulted in GWL drawdown of 7.5 mm day^{-1} during days without rainfall at our study site. During prolonged drought periods induced by climate extremes in 2019, when we observed only 45 mm rainfall during a consecutive 90-day period, the GWL fell to below −0.70 m, resulting in a large peat surface drop of −7.0 ± 1.3 cm in the intact sites (Extended Data Table 5). The peat surface had not rebounded from the 2019 perturbation by the end of the record, resulting in a total subsidence of −7.1 ± 2.4 cm during the period December 2017–May 2022 (Extended Data Table 5).

The close link between net rainfall (total rainfall minus evapotranspiration) and GWL (Extended Data Fig. 2) confirms that observed relatively low rainfall combined with increased seasonality and days without rainfall play a central role in shaping the seasonal and interannual variability of intact tropical peatland hydrology and therefore of CO_2 fluxes[7]. The El Niño[34] and positive Indian Ocean Dipole (IOD)[35] observations indicate that the region has experienced several moderate to very strong drought events in the recent past, suggesting that tropical peatland ecosystems are exposing and responding to changes in rainfall regime, which may limit their role as a carbon sink.

Given that GWLs at our intact forest site were slightly lower (annual rainfall = 1,883 mm $year^{-1}$; Extended Data Table 2) than those reported for a pristine peat swamp forest (annual rainfall = 2,880 mm $year^{-1}$)[7], we cannot entirely rule out some impact of surrounding land use on the hydrology and function of the peat dome as a whole. However, plantation water management is not believed to have affected forest hydrology at the flux tower footprint in the study area. Previous analysis suggested that such effects occurred within 300 m of the plantation boundary[25], and recent multivariate analysis indicates that subsidence in the interior forest is independent of distance from plantation canals[26]. This is further indicated by subsidence at rates of −1.4 cm $year^{-1}$ (Extended Data Table 5) observed at sampling locations between 7 to 10 km from the active plantation edge (Fig. 1). There was clearly a strong association during the study period between C loss, subsidence and droughts driven by regional climate extremes[26]. Our results indicate that even low-level or indirect human disturbance (for example, by means of climate change) can lead to C loss, highlighting the hydroclimatic vulnerability of C in forested tropical peatlands[13–16].

Other GHG fluxes and C loss

Net ecosystem exchanges of CH_4 (NEE-CH_4; net gaseous CH_4 exchange between ecosystem and atmosphere) were positive at all sites, but lower in the *Acacia* plantation and degraded site than in the intact site (Fig. 2 and Extended Data Table 4), consistent with lower GWLs promoting methanotrophy in the aerobic zone[27]. GWL drawdown below the root zone will also limit plant-mediated transport of CH_4 from the anaerobic zone to the atmosphere[27]. The finding that CH_4 emissions remained positive despite low GWLs (Fig. 3) may be attributed to emissions from vegetation and water surfaces[27].

Soil N_2O fluxes at the *Acacia* plantation were higher than at the degraded and intact sites (Fig. 2 and Extended Data Fig. 3), but were within the range of fluxes reported from oil palm plantation on peat[29,30]. Higher emissions from the plantation can be explained by a combination of leguminous *Acacia* trees that increase mineral nitrogen (N) availability through N fixation; accelerated mineralization of the peat under aerobic conditions (Extended Data Fig. 3) releasing mineral N as ammonium (Extended Data Table 1) and producing N_2O and nitrate during the nitrification process; and high availability of labile C and nitrate from rapid fine-root turnover (Extended Data Table 1), providing a substrate for denitrifier heterotrophs.

A previous study[36] within the same landscape reported fluvial C export of 0.3 ± 0.1 and 0.5 ± 0.1 tC ha^{-1} $year^{-1}$ in the intact and degraded sites, respectively. Owing to lack of fluvial C-export measurements for the *Acacia* plantation, we used a value of 0.4 ± 0.1 tC ha^{-1} $year^{-1}$ from a managed oil palm plantation in Southeast Asia[37]. Notably, fluvial C exports are fairly small compared with direct CO_2 emissions. We conservatively assume that all fluvial C export is ultimately emitted as CO_2 (ref. 38). The increased fluvial C export from the plantation and degraded forest may be attributed to enhanced mineralization with deeper GWL[37].

Finally, the measured aboveground and belowground biomass C stock was highest in the intact forest (aboveground biomass = 105.6 ± 21.7 tC ha^{-1} and belowground biomass = 24.8 ± 5.1 tC ha^{-1}) and decreased in the degraded forest (aboveground biomass = 88.7 ± 22.9 tC ha^{-1} and belowground biomass = 18.2 ± 4.7 tC ha^{-1}) and the *Acacia* plantation (aboveground biomass = 35.2 ± 1.9 tC ha^{-1} and belowground biomass = 7.2 ± 0.4 tC ha^{-1}, averaged over whole plantation rotation). Over a 100-year timescale (see Methods), biomass C losses owing to land-use change from intact forest were 0.9 ± 0.0 and 3.2 ± 0.9 tCO_2 ha^{-1} $year^{-1}$ in the degraded forest and *Acacia* plantation, respectively (Fig. 2 and Extended Data Table 4). Biomass C loss owing to plantation establishment on degraded forest was 2.4 ± 0.9 tCO_2 ha^{-1} $year^{-1}$ (Extended Data Table 4).

Net GHG balance of *Acacia* plantation

Comparison of GHG fluxes at the *Acacia* plantation and degraded and intact sites in this tropical peat landscape indicates that conversion of intact forest to *Acacia* plantation or degraded forest results in a substantial increase in CO_2 and N_2O emissions and a decrease in CH_4 emissions. Overall, the associated warming impact of higher CO_2 and N_2O emissions is larger than the accompanying cooling impact of lower CH_4 emissions (Fig. 2). We calculated total GHG balances of all sites using a sustained-flux global-warming potential of 1, 45 and 270 for CO_2, CH_4 and N_2O, respectively, over a 100-year time period[39]. The GHG balance and the subsidence rate in the *Acacia* plantation were around two times higher than those measured at the intact site (Fig. 2 and Extended Data Table 5). The measured CO_2 emissions in this study indicate that the long-term rate of C accumulation of 2.8 tCO_2 ha^{-1} $year^{-1}$ in the Kampar Peninsula[8] may no longer be occurring. If we take the measured GHG balance of the intact forest site as a reference, and treat our data from the fourth *Acacia* rotation as representative of longer-term conditions, then the conversion of intact site to *Acacia* plantation results in a long-term net increase in GHG emissions of 18.1 ± 6.0 tCO_2-eq ha^{-1} $year^{-1}$ (Fig. 2).

Our study is the first, to our knowledge, to provide an estimate of CO_2 emissions from tropical *Acacia* plantation on peat based on the eddy covariance method, over a full plantation rotation. The CO_2 EF is critical to GHG inventories in *Acacia* plantations, given that, in *Acacia*

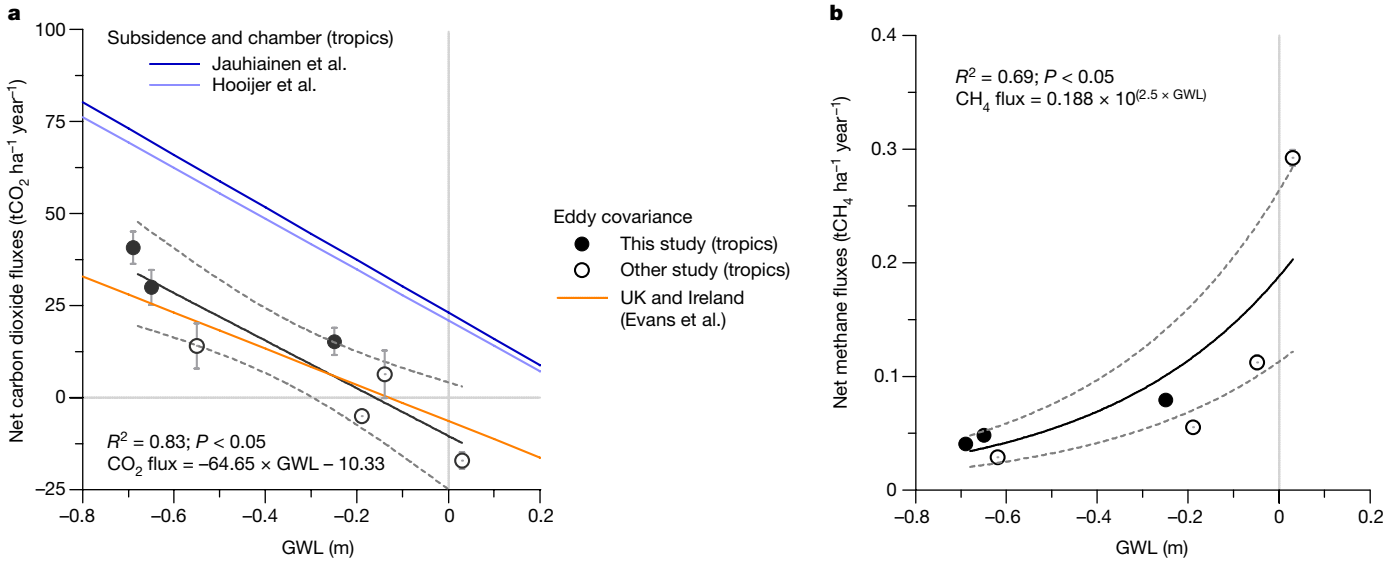

Fig. 3 | GWL controls carbon dioxide and methane fluxes in tropical peatlands. a, Carbon dioxide (CO_2). **b**, Methane (CH_4). Relationship between net CO_2 and CH_4 fluxes and GWL were derived from published eddy covariance flux studies in tropical peatlands. The solid lines show the best-fit models and the dashed lines show 95% confidence intervals. The statistical test used a significance level of 5%. Positive values indicate net emission to the atmosphere, negative values indicates net uptake by the ecosystem. CO_2 results are compared with a previous relationship between CO_2 fluxes and GWL derived from subsidence[22] and soil flux chamber[23] measurements and a relationship for peatlands in the United Kingdom and Ireland[45] is based on eddy covariance measurements. Positive and negative GWL values indicate the water level above and below the peat hollow surface, respectively.

plantation, about 90% of peat on-site GHG emissions is released as CO_2 (Fig. 2). We were able to reduce the uncertainties associated with variations in flux during the full plantation rotation and in biomass removal at the end of the rotation, which make estimating the average C balance of high-latitude peatlands with multidecadal rotations highly problematic. Our directly measured CO_2 balance of the *Acacia* plantation is half of the IPCC Tier 1 EF value of 73 tCO_2 ha^{-1} $year^{-1}$. Two of the key studies[22,23] used to derive the Tier 1 EF were carried out in the same plantation area in the initial 3–8 years after drainage, so interregional differences cannot explain the discrepancy. Subsidence rates[24,26,40] and CO_2 emissions[30,41,42] in tropical peatlands are reported to decrease over time following drainage. An increase in bulk density (0.08 g cm^{-3} during 3–8 years after drainage in refs. 22,23 versus 0.20 g cm^{-3} during 17–22 years after drainage in this study; Extended Data Table 1), owing to peat compaction during land preparation, may result in lower peat oxidative decomposition because of the increase in soil water content and decrease in soil gas diffusivity[43]. Furthermore, a decline in soil organic matter quality[44] and nutrient availability over time may leave behind a more stable peat matrix, resulting in a decrease in substrate-driven rates of CO_2 production[41] from peat decomposition. Finally, not all of the emissions in the initial years after plantation establishment[22,23] would come directly from peat C decomposition, given that considerable forest biomass residues would also contribute to the initial CO_2 loss, with most[42] of the forest residues decomposing in the initial years after conversion.

Some other factors may have contributed to lower than expected long-term plantation emissions in our study. Improved water management practices, reflected in higher average GWL than reported in previous studies[22,23], may have reduced oxidation rates to some extent. We also measured a C input to the peat of around 12 tCO_2 ha^{-1} $year^{-1}$ (calculated as the difference between the oxidative peat decomposition (41.7 tCO_2 ha^{-1} $year^{-1}$; Extended Data Table 3) and the sum of NEE-CO_2 (9.5 tCO_2 ha^{-1} $year^{-1}$) and C export in harvested wood (20.5 tCO_2 ha^{-1} $year^{-1}$)) over the full plantation rotation. This C input, derived from litter, roots, stumps and bark residues, is not measured during chamber and subsidence studies, which may have led to overestimation of net CO_2 emissions. Although our results confirm that fibre wood plantations are substantial net GHG sources, these results indicate that there may be opportunities to increase soil C input through better post-harvest residue management. Further research is needed to confirm the potential scale of increase in C input that could realistically be achieved.

The data from our three study sites, along with four other published eddy covariance studies from tropical peatlands (Extended Data Table 6), conform well to a linear relationship between CO_2 flux and GWL (R^2 = 0.83, P < 0.05; Fig. 3), suggesting that measured emissions are broadly consistent with those of other studies that applied a similarly rigorous whole-ecosystem eddy covariance measurement approach. As is evident from Fig. 3, net CO_2 fluxes and their relationships with GWL derived from eddy covariance studies are substantially lower than those obtained from chamber and subsidence studies in the same ecosystems. Although the number of published eddy covariance studies from tropical peatlands remains insufficient to establish whether these differences are systematic, a similar offset is evident in CO_2 flux versus GWL relationships derived from eddy covariance data[45] and chamber data[46] for high-latitude peatlands. Although further data are needed, we therefore tentatively conclude that emissions from *Acacia* plantation are substantially lower than the current IPCC Tier 1 EFs, as a result of methodological limitations to the data available at the time of publication of the IPCC Wetlands Supplement[20] and changes in peat physicochemical properties with time since drainage.

Our results should not be extrapolated to other agriculture on peat in the region (for example, sago, oil palm, rubber plantations etc.) or to other tropical peatlands, such as those of the Amazon and Congo basins, because they have different rainfall regimes, vegetation and peat-formation histories. Nevertheless, the strong linear relationship between CO_2 flux and GWL shown in Fig. 3 does suggest that, when the average annual GWL is known, the peatland CO_2 balance can be predicted with some degree of confidence. This is in line with work[45,47] on high-latitude peatlands suggesting that GWLs are more important than local climate or other management factors. Furthermore, although the relationship between CO_2 flux and GWL is steeper for tropical peatlands compared with the full set of high-latitude flux tower data collated in ref. 45, we found less difference than expected between the tropical

data and the data presented from the UK and Irish sites in the same study (Fig. 3). This finding is in marked contrast to a recently published synthesis study suggesting that tropical peatlands are inherently more sensitive to CO_2 loss following GWL drawdown[48]. However, given that ref. 48 incorporated the same chamber studies used to derive the IPCC Tier 1 EF, we believe that it may have overestimated rates of CO_2 loss from tropical peatlands for the same reasons noted above.

Using our EFs, net GHG emissions from *Acacia* plantations on peat in Indonesia are calculated to be 20 Mt CO_2-eq $year^{-1}$ (based on the area of *Acacia* plantation on peat in Indonesia, 1.12×10^6 ha (ref. 21)). This equates to 1.1% of Indonesia's most recently reported total GHG emissions in 2019 (ref. 49). Infrequent but intense fires are common in unmanaged degraded peatlands, particularly during prolonged drought driven by climate extreme events (for example, 2006, 2015 and 2019), and may result in higher GHG release to the atmosphere than peat decomposition[49]. GHG emissions at the degraded site are about 20% higher than those of the plantation site, indicating that establishment of *Acacia* plantation on previously degraded site could apparently result in lower long-term GHG emissions of -7.5 ± 6.5 tCO_2-eq ha^{-1} $year^{-1}$, as well as avoided emissions from bioenergy production (Fig. 2). Because the initial disturbance of this site occurred at a similar time to that at the plantation site (see Methods), it is probable that higher emissions from the degraded site are partly because of the decomposition of woody debris from fallen dead trees. Our results do not argue against full restoration of unmanaged degraded peatlands where this is achievable, as their ecosystem rehabilitation (that is, hydrological restoration and re-establishment of a closed forest canopy) offers an opportunity to restore and improve the ability of peatlands to sequester and retain C, but this will be critically dependent on protecting these areas from encroachment and fire.

Using our EFs from the intact and degraded sites, the results highlight that, despite evidence that they may now be losing C, avoided emissions from conserving all remaining intact peat swamp forests in Indonesia (2.0×10^6 ha) under Indonesia's nationally determined contribution[49] and emissions reduction from restoring 4.2×10^6 ha by 2050 under Indonesia's Low Carbon scenario Compatible with the Paris Agreement target (LCCP)[50] will avoid GHG emissions of around 160 $MtCO_2$-eq $year^{-1}$. This equates to around 40% of GHG emissions from peat decomposition in Indonesia in 2019 (ref. 49). This estimate is conservative. If some remaining intact peatlands are continuing to sequester CO_2, the avoided emissions will be correspondingly higher. Our results clearly indicate that the net avoidance and reduction of GHG emissions resulting from peatland conservation, restoration and sustainable management represent a notable contribution to nationally determined contributions to a 1.5 °C world[32].

Online content

Any methods, additional references, Nature Portfolio reporting summaries, source data, extended data, supplementary information, acknowledgements, peer review information; details of author contributions and competing interests; and statements of data and code availability are available at https://doi.org/10.1038/s41586-023-05860-9.

1. Lähteenoja, O. et al. The large Amazonian peatland carbon sink in the subsiding Pastaza-Marañón foreland basin, Peru. *Glob. Change Biol.* **18**, 164–178 (2012).
2. Dargie, G. C. et al. Age, extent and carbon storage of the central Congo Basin peatland complex. *Nature* **542**, 86–90 (2017).
3. Warren, M., Hergoualc'h, K., Kauffman, J. B., Murdiyarso, D. & Kolka, R. An appraisal of Indonesia's immense peat carbon stock using national peatland maps: uncertainties and potential losses from conversion. *Carbon Balance Manag.* **12**, 12 (2017).
4. Gumbricht, T. et al. An expert system model for mapping tropical wetlands and peatlands reveals South America as the largest contributor. *Glob. Change Biol.* **36**, 335 (2017).
5. Kurnianto, S. et al. Carbon accumulation of tropical peatlands over millennia: a modeling approach. *Glob. Change Biol.* **21**, 431–444 (2015).
6. Dommain, R., Couwenberg, J. & Joosten, H. Development and carbon sequestration of tropical peat domes in south-east Asia: links to post-glacial sea-level changes and Holocene climate variability. *Quat. Sci. Rev.* **30**, 999–1010 (2011).
7. Cobb, A. R. et al. How temporal patterns in rainfall determine the geomorphology and carbon fluxes of tropical peatlands. *Proc. Natl Acad. Sci. USA* **114**, E5187–E5196 (2017).
8. Hapsari, K. A., Jennerjahn, T., Nugroho, S. H., Yulianto, E. & Behling, H. Sea level rise and climate change acting as interactive stressors on development and dynamics of tropical peatlands in coastal Sumatra and South Borneo since the Last Glacial Maximum. *Glob. Change Biol.* **28**, 3459–3479 (2022).
9. Gallego-Sala, A. V. et al. Latitudinal limits to the predicted increase of the peatland carbon sink with warming. *Nat. Clim. Change* **8**, 907–913 (2018).
10. Loisel, J. et al. Expert assessment of future vulnerability of the global peatland carbon sink. *Nat. Clim. Change* **11**, 70–77 (2021).
11. Wang, S., Zhuang, Q., Lähteenoja, O., Draper, F. C. & Cadillo-Quiroz, H. Potential shift from a carbon sink to a source in Amazonian peatlands under a changing climate. *Proc. Natl Acad. Sci.* **115**, 12407–12412 (2018).
12. Li, W. et al. Future precipitation changes and their implications for tropical peatlands. *Geophys. Res. Lett.* **34**, L01403 (2007).
13. Dadap, N. C. et al. Climate change-induced peatland drying in Southeast Asia. *Environ. Res. Lett.* **17**, 074026 (2022).
14. Dommain, R., Couwenberg, J., Glaser, P. H., Joosten, H. & Suryadiputra, I. N. N. Carbon storage and release in Indonesian peatlands since the last deglaciation. *Quat. Sci. Rev.* **97**, 1–32 (2014).
15. Garcin, Y. et al. Hydroclimatic vulnerability of peat carbon in the central Congo Basin. *Nature* **612**, 277–282 (2022).
16. Swails, E. et al. The response of soil respiration to climatic drivers in undrained forest and drained oil palm plantations in an Indonesian peatland. *Biogeochemistry* **142**, 37–51 (2019).
17. Deshmukh, C. S. et al. Conservation slows down emission increase from a tropical peatland in Indonesia. *Nat. Geosci.* **14**, 484–490 (2021).
18. Leifeld, J. & Menichetti, L. The underappreciated potential of peatlands in global climate change mitigation strategies. *Nat. Commun.* **9**, 1071 (2018).
19. Austin, K. G. et al. A review of land-based greenhouse gas flux estimates in Indonesia. *Environ. Res. Lett.* **13**, 055003 (2018).
20. Drösler, M. et al. in *2013 Supplement to the 2006 IPCC Guidelines for National Greenhouse Gas Inventories: Wetlands* (eds Hiraishi, T. et al.) 2.1–2.79 (IPCC, 2013).
21. Miettinen, J., Shi, C. & Liew, S. C. Land cover distribution in the peatlands of Peninsular Malaysia, Sumatra and Borneo in 2015 with changes since 1990. *Glob. Ecol. Conserv.* **6**, 67–78 (2016).
22. Hooijer, A. et al. Subsidence and carbon loss in drained tropical peatlands. *Biogeosciences* **9**, 1053–1071 (2012).
23. Jauhiainen, J., Hooijer, A. & Page, S. E. Carbon dioxide emissions from an *Acacia* plantation on peatland in Sumatra, Indonesia. *Biogeosciences* **9**, 617–630 (2012).
24. Hoyt, A. M., Chaussard, E., Seppalainen, S. S. & Harvey, C. F. Widespread subsidence and carbon emissions across Southeast Asian peatlands. *Nat. Geosci.* **13**, 435–440 (2020).
25. Evans, C. D. et al. Rates and spatial variability of peat subsidence in *Acacia* plantation and forest landscapes in Sumatra, Indonesia. *Geoderma* **338**, 410–421 (2019).
26. Evans, C. D. Long-term trajectory and temporal dynamics of tropical peat subsidence in relation to plantation management and climate. *Geoderma* **428**, 116100 (2022).
27. Deshmukh, C. S. et al. Impact of forest plantation on methane emissions from tropical peatland. *Glob. Change Biol.* **26**, 2477–2495 (2020).
28. Wong, G. X. et al. How do land use practices affect methane emissions from tropical peat ecosystems? *Agric. For. Meteorol.* **107869**, 282–283 (2020).
29. Swails, E., Hergoualc'h, K., Verchot, L., Novita, N. & Lawrence, D. Spatio-temporal variability of peat CH_4 and N_2O fluxes and their contribution to peat GHG budgets in Indonesian forests and oil palm plantations. *Front. Environ. Sci.* **9**, 617828 (2021).
30. Swails, E., Hergoualc'h, K., Deng, J., Frolking, S. & Novita, N. How can process-based modeling improve peat CO_2 and N_2O emission factors for oil palm plantations?. *Sci. Total Environ.* **839**, 156153 (2022).
31. Prairie, Y. T. et al. Greenhouse gas emissions from freshwater reservoirs: what does the atmosphere see? *Ecosystems* **21**, 1058–1071 (2018).
32. Roe, S. et al. Contribution of the land sector to a 1.5 °C world. *Nat. Clim. Change* **9**, 817–828 (2019).
33. Ruwaimana, M., Anshari, G. Z., Silva, L. C. R. & Gavin, D. G. The oldest extant tropical peatland in the world: a major carbon reservoir for at least 47 000 years. *Environ. Res. Lett.* **15**, 11 (2020).
34. Cai, W. et al. Increasing frequency of extreme El Niño events due to greenhouse warming. *Nat. Clim. Change* **4**, 111–116 (2014).
35. Cai, W. et al. Increased frequency of extreme Indian Ocean Dipole events due to greenhouse warming. *Nature* **510**, 254–258 (2014).
36. Yupi, H. M., Inoue, T., Bathgate, J. & Putra, R. Concentrations, loads and yields of organic carbon from two tropical peat swamp forest streams in Riau Province, Sumatra, Indonesia. *Mires Peat* **18**, 1–15 (2016).
37. Cook, S. et al. Fluvial organic carbon fluxes from oil palm plantations on tropical peatland. *Biogeosciences* **15**, 7435–7450 (2018).
38. Evans, C. D., Renou-Wilson, F. & Strack, M. The role of waterborne carbon in the greenhouse gas balance of drained and re-wetted peatlands. *Aquat. Sci.* **78**, 573–590 (2016).
39. Neubauer, S. C. & Megonigal, J. P. Moving beyond global warming potentials to quantify the climatic role of ecosystems. *Ecosystems* **18**, 1000–1013 (2015).
40. Umarhadi, D. A. et al. Tropical peat subsidence rates are related to decadal LULC changes: insights from InSAR analysis. *Sci. Total Environ.* **816**, 151561 (2022).
41. Swails, E. et al. Will CO_2 emissions from drained tropical peatlands decline over time? Links between soil organic matter quality, nutrients, and C mineralization rates. *Ecosystems* **21**, 868–885 (2018).
42. McCalmont, J. et al. Short- and long-term carbon emissions from oil palm plantations converted from logged tropical peat swamp forest. *Glob. Change Biol.* **27**, 2361–2376 (2021).
43. Melling, L., Goh, K. J., Chaddy, A. & Hatano, R. Soil CO_2 fluxes from different ages of oil palm in tropical peatland of Sarawak, Malaysia as influenced by environmental and soil properties. *Acta Hortic.* **982**, 25–35 (2013).

44. Hoyos-Santillan, J. et al. Quality not quantity: organic matter composition controls of CO_2 and CH_4 fluxes in neotropical peat profiles. *Soil Biol. Biochem.* **103**, 86–96 (2016).
45. Evans, C. D. et al. Overriding water table control on managed peatland greenhouse gas emissions. *Nature* **593**, 548–552 (2021).
46. Tiemeyer, B. et al. A new methodology for organic soils in national greenhouse gas inventories: data synthesis, derivation and application. *Ecol. Indic.* **109**, 105838 (2020).
47. Ma, L. et al. A globally robust relationship between water table decline, subsidence rate, and carbon release from peatlands. *Commun Earth Environ* **3**, 254 (2022).
48. Zou, J. et al. Rewetting global wetlands effectively reduces major greenhouse gas emissions. *Nat. Geosci.* **15**, 627–632 (2022).
49. Ministry of Environment and Forestry. Indonesia. Third Biennial Update Report. Under the United Nations Framework Convention on Climate Change (2021).
50. Government of Indonesia. Indonesia. Long-Term Strategy for Low Carbon and Climate Resilience 2050 (2021).

Methods

Study area

This study was conducted in the Kampar Peninsula (Sumatra, Indonesia), an ombrogenous tropical peatland of around 700,000 ha that largely formed within the past 5,100 years (ref. 8). The base of the peatland is grey marine clays, over which peat varies from approximately 3 m deep near the river boundaries to over 11 m in the centre of the approximately 60-km-wide and more than 100-km-long peat dome (Fig. 1), with an average depth of 8 m. The peninsula experiences a humid tropical climate with the average monthly air temperature ranging from 26 to 29 °C (refs. 17,27). The variability in rainfall is influenced by monsoonal processes combined with El Niño–Southern Oscillation and IOD[51,52]. In general, the El Niño[34] and positive IOD[35] occur sequentially, with the positive IOD peaking a few months after the El Niño, exerting a strong combined effect on regional rainfall patterns[26]. The average annual rainfall for the past 8 years (2014–2021, with El Niño in 2015, La Niña in 2017 and a major positive IOD combined with an El Niño event in 2019) is 1,772 ± 201 mm. Rainfall varies seasonally, with two annual peaks, one in November–December and another in March–April. The land cover of the peninsula is characterized by a large central forest area that still has good-quality dense forest, representing one of the largest peat swamp forests in Southeast Asia. In some parts of the peninsula, selective logging took place in the 1990s, including the construction of access logging tracks and canals, especially around the periphery of the forest. However, some areas have never been logged and have been classified as intact peat swamp forest[21]. Most of the logged forest was converted to industrial fibre wood plantation and smallholder agriculture in the early 2000s. At present, the central forest area is surrounded by a mosaic of *A. crassicarpa*, oil palm plantation and degraded peat swamp forest with shrub and open land[21] (Fig. 1).

At the experimental fibre wood plantation site, the peat swamp forest was disturbed by selective logging activity, including logging tracks and canals in the early 1990s. In the early 2000s, the area was converted to an *Acacia* plantation. This involved clearance of the remaining logged forest, artificial compaction during mechanical land preparation, installation of regularly spaced water management and access canals and planting of *A. crassicarpa*, which is harvested on a 4–5-year rotation. The area was not affected by fire before, during or after land-use change. *Acacia crassicarpa* (Leguminosae) is a fast-growing, N-fixing tree that is the principal fibre wood plantation species grown on peat soils in Southeast Asia. The typical plantation rotation period between planting of tree seedlings to harvest is 4–5 years, and a closed canopy develops in around 12 to 18 months. When measurements began in October 2016, the trees were already at the end of the third plantation rotation. All plantation compartments within a 2-km radius around the eddy covariance tower were harvested between October 2016 and April 2017. Tree height at harvest was in the range 19–24 m, determined from a vegetation survey in permanent sampling plots (20 m × 125 m) around the tower. Replanting for the fourth plantation rotation took place within two weeks after harvesting each individual compartment at a density of 1,667 trees per hectare (3 m × 2 m spacing). Five grams of chelated micronutrients per tree were applied around the seedlings during planting. All compartments within a 2-km radius of the eddy covariance tower were harvested between June and August 2021, when the average plantation age was 4.7 years, and replanting for the fifth plantation rotation took place within two weeks after harvesting. The ground surface in the plantation area is relatively even, without a hummock-hollow microtopography and with very little understory vegetation. The site soil characteristics are summarized in Extended Data Table 1. GWLs in the experimental plantation are actively managed by means of an extensive network of topographically defined water management zones, controlled by outlet sluices and supported by GWL monitoring. Water management zones consist of navigable canals, typically of 12 m width and 3 m depth, also used for transport[25]. Branch canals of 5–8 m width run perpendicular to these canals at a spacing of 500–800 m to form plantation compartments, which contain 1-m-deep field drains at a spacing of 75 m (ref. 25). An integrated climatologic footprint analysis[53] indicated that (1) approximately 80% of measured fluxes derived from within 1,000 m in the upwind direction and thus originated within the *Acacia* plantation and (2) the water surface of ditches and canals represented 2% of the flux footprint (Fig. 1).

The second eddy covariance tower is located on the boundary of the degraded peatland and *Acacia* plantation (Fig. 1). To represent only the degraded peatland, half-hourly measurements in which the prevailing wind came from the plantation site (90° to 270°) were excluded, as is commonly done in eddy covariance studies[54]. The degraded site was selectively logged and drained in the late 1990s and early 2000s, whereas some parts were burned in 2014. The average canopy height was about 19 m. The tree density with a diameter at breast height of greater than 5 cm was 663 trees per hectare. Some large trees had been logged or fallen and many of those remaining were leaning. The site characteristics are summarized in Extended Data Table 1. The integrated climatologic footprint analysis[53] indicated that approximately 80% of the fluxes were derived within 1,000 m in the upwind direction and the previously burnt area represented around 5% of the flux footprint (Fig. 1). The average eddy covariance footprint can be considered typical of many unmanaged degraded peatlands in Southeast Asia[21].

The intact peat swamp forest structure is mixed with an uneven canopy (average canopy height = 32 m). The density of trees with a diameter at breast height greater than 5 cm was 1,343 stems per hectare. The vegetation and soil characteristics are summarized in Extended Data Table 1. The GWL fluctuates following the rainfall variation because of the ombrotrophic nature of the area[17,27]. An integrated climatologic footprint analysis[53] indicated that approximately 80% of the fluxes were derived within 1,000 m in the upwind direction (Fig. 1) and thus originated from intact forest with neither logging nor canal-construction activity[21]. Some long-term regional effects of hydrological management of surrounding plantations cannot be ruled out, but a previous analysis suggested that the strongest effects occurred within 300 m of the plantation boundary[25], and recent multivariate analysis indicates that subsidence in the interior forest is independent of distance from plantation canals[26]. The nearest active plantation is 3.5 km from the flux tower and well outside the flux footprint. Further, to avoid any possible boundary effect and associated bias, measurements from a wind direction between 78° and 191° were excluded in this study (Fig. 1).

Eddy covariance provides half-hourly measurements of turbulent exchanges between an entire ecosystem and the atmosphere above the vegetation canopy[54]. Hence, eddy covariance measurements incorporate all existing sources and uptakes that can vary substantially within an ecosystem in both space and time arising from variation in environmental conditions. Given the flat terrain (slope less than 0.05%), using the measured vegetation-canopy height and wind speed, the estimated 80% eddy covariance flux footprints represent an area of interest of around 1,000 m radius (Fig. 1). Flux measurements with the eddy covariance technique are expensive and high maintenance, and few studies include replicated measurements from several towers in tropical forested ecosystems. The relatively close proximity of the *Acacia* plantation and intact and degraded sites (Fig. 1) within the same peat landscape avoids potentially confounding variables such as differences in past natural succession[55] and peat formation[8].

Eddy covariance and environmental variable measurements

Each eddy covariance system consisted of an enclosed-path CO_2/H_2O analyser (LI-7200, LI-COR) to measure CO_2 and H_2O concentrations, an open-path CH_4 analyser (LI-7700, LI-COR) to measure CH_4 concentrations and a three-dimensional sonic anemometer (WindMaster Pro 3-Axis Anemometer, Gill Instruments) to measure the orthogonal components of wind-speed fluctuations. Eddy covariance sensors were

mounted at the top of each tower to ensure complete exposure in all directions (Fig. 1). The filters of the CO_2 analyser were manually cleaned, either biweekly or if the flow drive increased above 80% (indicating filter clogging). The mirrors of the CH_4 analyser were cleaned automatically either at 05:00 local time every day or if the received-signal-strength indicator dropped below 20%, because CH_4 data become noisy below this threshold. Furthermore, the upper and lower mirrors of the CH_4 analyser were manually cleaned on a biweekly basis. The raw eddy covariance turbulence data were recorded at 10 Hz using an analyser interface unit (LI-7550, LI-COR) and were stored on a removable flash disk (Industrial Grade USB Flash Disk, APRO).

A quantum sensor (LI-190SL-50, LI-COR) was mounted at the top of each tower to measure incoming photosynthetic photon flux density (PPFD). A radiometer (CNR4, Kipp & Zonen) was also mounted at the top of each tower to measure global and net radiation. Vertical profiles of relative humidity and air temperature were measured using air-temperature and humidity probes (HMP155, Vaisala), which were installed inside ventilated radiation shields at five heights from the ground surface, 3, 7, 13, 23 and 40 m for the plantation site, 3, 7, 14, 21 and 40 m for the degraded site and 4, 11, 20, 29 and 48 m for the intact site. Vertical profiles of the CO_2 concentrations were measured by air sampling at four heights, 3, 12, 22 and 40 m for the plantation site, 3, 14, 21 and 40 m for the degraded site and, 4, 11, 29 and 48 m for the intact site, to calculate the flux-storage[56] term below the measurement height using a closed-path CO_2 analyser (LI-8100, LI-COR). The air-sampling intakes were automatically changed every 90 s and the CO_2 concentration was measured for the last 10 s of every 90-s sampling time at each sampling height and recorded using a data logger (LI-8100, LI-COR); therefore, one rotation of measurements took 6 min in every 30 min. Both the enclosed-path and closed-path CO_2 analysers were calibrated every three months using reference gases with concentrations of 396 and 444 ppm CO_2 in air (certified grade ±1 ppm) and ultrahigh-purity nitrogen as the zero-point gas. The soil temperature was measured at 0.15 m below the hollow peat surface using a temperature probe (HydraProbe II, Stevens Water Monitoring Systems) from September 2017 until November 2018 and from October 2016 until June 2020 with three replicates at the intact and plantation sites, respectively. From November 2019 until May 2022, the soil temperatures were measured at the intact site and from November 2019 until May 2021 at the plantation site with two replicates using a temperature probe (AquaCheck, South Africa). The soil temperatures were not measured at the degraded site owing to site logistic issues.

All meteorological sensors took measurements every second and were recorded as 1-min averages using a data logger (Model 9210 XLite, Sutron). Each measuring system was powered using five solar panels (65-W solar panel, SunWize), along with eight rechargeable batteries (6 V and 305 Ah, Sun Xtender). The daily rainfall (mm day^{-1}) was manually measured using three, two and three bucket-rain gauges within a distance of 11 km from the tower location at the plantation, degraded and intact sites, respectively. Each rain gauge was installed 1.5 m above the ground, in an open area so that rainfall was not affected by surrounding vegetation.

The GWL was monitored as the water elevation relative to the ground surface, taking the base of the hollows as a datum[17]. Data were recorded as negative distance below the surface, with positive values indicating ponding above the surface. The GWL loggers (four around the plantation tower, one in the degraded site and six in the intact site) to record the GWL every 30 min using a pressure transducer (Levelogger Model 3001, Solinst) were placed in perforated polyvinyl chloride pipes that were inserted vertically into the peat and anchored into the underlying clay (Fig. 1). Each GWL logger also recorded the water temperature in the pipe 1.5 m below the peat surface. Further GWL data were manually recorded biweekly at seven and three locations at the plantation and degraded sites, respectively, and on a quarterly basis at eight more locations in the intact site (Fig. 1).

Peat subsidence was measured at 11, four and 14 locations in the plantation, degraded and intact sites, respectively (Fig. 1), with hollow, perforated 5-cm-diameter polyvinyl chloride poles inserted vertically into the peat and anchored into the underlying mineral subsoil following the approach described in ref. 25. Annual average subsidence rates were derived from measurements during October 2016–May 2021 for the plantation site and during December 2017–May 2022 for the degraded and intact sites.

For peat physical and chemical properties of the surface layer (0–50 cm), four plots in each of the *Acacia* plantation and degraded sites and three plots in the intact site were randomly selected within the eddy covariance flux footprint (200–1,000 m distance from each tower location; Fig. 1). At each plot, ten subsamples within a 200-m radius were composited. Peat samples for bulk density, pH and ash content were collected in September 2017, February 2019 and September 2019 in the intact site, June 2017, January 2018, October 2018 and February 2019 in the degraded site and June 2017, February 2018, October 2018, February 2019 and October 2019 in the *Acacia* plantation. Samples for soil C, N, nitrate and ammonium content were collected in August 2020 and October 2021 for all sites.

For the *Acacia* plantation site, time-integrated NEE-CO_2 over the plantation rotation was combined with C export in the harvested wood. Total C export in harvested wood and delivered to the mill from the total footprint area of 220 ha over the average plantation age of 4.7 years was calculated using a basic density of 455 ± 25 kg m^{-3} and average C content of 48.2% (refs. 56–59). The exported wood is converted into pulp products and biomass fuel for bioenergy generation. We applied the conservative assumption that all C in exported wood would be returned to the atmosphere as CO_2. Intact and degraded sites were considered to have had no biomass C export during the study period.

The biomass C loss owing to land-use change was calculated from aboveground and belowground biomass C-stock differences between the intact site and the *Acacia* plantation and degraded areas. Aboveground and belowground biomass were determined using seven permanent sampling plots (20 m × 125 m) at each site and following the allometric equations described in refs. 60,61 for the intact and degraded sites and ref. 62 for the *Acacia* plantation. A time horizon of 100 years of land being used after conversion is chosen on the basis of ISO 14067 on C footprint.

Eddy covariance data processing

The eddy covariance fluxes of CO_2, CH_4 and evapotranspiration were computed from the 10-Hz concentration and vertical wind velocity data using EddyPro software (version 6.2.0, LI-COR) at a standard half-hour averaging interval[54]. A despiking procedure was applied to detect and eliminate individual out-of-range values for vertical wind velocity and concentration data[63]. Detrending was carried out using the block-averaging method. A coordinate correction was applied to force the average vertical wind velocity to zero by the planar-fit method[64]. Frequency response loss corrections were applied to compensate for the flux losses at low and high frequencies[65]. The Webb–Pearman–Leuning correction[66] for air-density fluctuations induced by temperature (thermal expansion) and water vapour (dilution) was applied.

Differences between deployment-specific variables, that is, the sensor separation distance and instrument placement, were considered when processing the data. The half-hourly CO_2 storage below the flux measurement height was calculated from the four-point vertical profiles of CO_2 concentration, relative humidity and air temperature by temporal interpolation[56]. Finally, the net ecosystem CO_2 exchange was calculated as the sum of the storage flux and the eddy covariance flux. Owing to the large power requirement and cost of a separate CH_4 analyser, we could not conduct CH_4-profile measurements to calculate the CH_4 storage[67]. In theory, accumulated CH_4 below the canopy during the nighttime is probably released and measured by the eddy covariance system following the onset of turbulence after sunrise, and the bias on annual sums should be negligible[67].

After a set of quality controls[68–70] and system malfunctions and power-supply failure mainly because of lightning strikes, the numbers of high-quality measurements during the course of the study were 37%, 34% and 34% for CO_2, 26%, 29% and 25% for CH_4 and 34%, 34% and 28% for evapotranspiration in the plantation, degraded and intact sites, respectively. A similar range of 25–50% has been reported for other eddy covariance studies in tropical forested peatlands[42,56]. The remaining half-hourly measurements that met all the quality criteria totalled 30,196, 14,330 and 18,136 for CO_2, 21,305, 12,721 and 13,026 for CH_4 and 27,965, 14,437 and 14,919 for evapotranspiration for the plantation, degraded (270–90° wind direction) and intact (191–78° wind direction) sites, respectively.

We gap-filled both low-quality and missing data, as is commonly done in eddy covariance studies[17,27,42,56,71–75]. Following ref. 17, we applied three gap-filling approaches for CO_2: (1) marginal distribution sampling (MDS)[56,76], (2) artificial neural network (ANN)[73] and (3) random forest (RF)[74] separately for the daytime (06:00–18:00 local time) and the nighttime (18:00–06:00 local time) data. To avoid any possible gap-filling bias in estimates of CO_2, CH_4 and evapotranspiration, we used the average of the three approaches[17]. We applied principal component analysis as an input to the algorithms to address multidriver dependency of CO_2 exchange and reduce the internal complexity of the algorithmic structures for the MDS approach[77], using PPFD, vapour-pressure deficit (VPD) and air temperature during daytime. Nighttime CO_2 exchanges were considered equivalent to the ecosystem respiration (R_{eco}) value[78]. The GWL is reported as the main controlling factor of R_{eco} from tropical peatlands[17,56]. Therefore, we used the GWL, air temperature and soil temperature as environmental factors for the lookup table to derive the nighttime CO_2 exchanges using the MDS gap-filling algorithm. Following other regional eddy covariance studies in peat swamp forests[17,56], we performed MDS gap-filling using the REddyProc package (https://CRAN.R-project.org/package=REddyProc) on a half-hourly basis[77]. ANN and RF procedures were iterated 20 times. For ANN and RF, PPFD, VPD, air temperature, GWL and friction velocity were used as predictive variables for the daytime and the PPFD and VPD data were excluded in the nighttime.

We applied the above gap-filling approaches for CH_4 and evapotranspiration as well. For CH_4, we used GWL, VPD, air temperature, friction velocity, latent heat flux, sensible heat flux, atmospheric pressure and global radiation in the daytime and latent heat flux and global radiation were excluded in the nighttime for ANN and RF. For MDS, we used latent heat flux, GWL and air temperature during the daytime and GWL, air temperature and soil temperature during the nighttime. For evapotranspiration, we applied net radiation instead of PPFD during the daytime, whereas net radiation and VPD were excluded during the nighttime. After gap filling, we corrected the daily evapotranspiration for the energy imbalance using net radiation, sensible heat and latent heat as described in ref. 79.

The flux random uncertainty was calculated following ref. 80. The standard deviation of three different flux values derived from friction velocity thresholds of the 5th, 50th and 95th percentiles were applied as an uncertainty because of the friction velocity threshold using the REddyProc package[77]. The gap-filling flux uncertainty was calculated from the standard deviation of the MDS procedure[77]. Averages of the 20 ANN and RF modelled values were used to fill gaps and the standard deviation was used to quantify the uncertainty owing to gap filling. The total uncertainty in eddy covariance measurements of CO_2, CH_4 and evapotranspiration included gap-filling, random and friction velocity uncertainty[81]. The annual estimate of CO_2, CH_4, evapotranspiration and GHG balance includes total uncertainty calculated using the propagation of errors law.

Reporting summary

Further information on research design is available in the Nature Portfolio Reporting Summary linked to this article.

Data availability

All data that support the findings of this study are archived on Zenodo at https://doi.org/10.5281/zenodo.7728463.

51. Saji, N. H., Goswami, B. N., Vinayachandran, P. N. & Yamagata, T. A dipole mode in the tropical Indian Ocean. *Nature* **401**, 360–363 (1999).
52. Alsepan, G. & Minobe, S. Relations between interannual variability of regional-scale Indonesian precipitation and large-scale climate modes during 1960–2007. *J. Climate* **33**, 5271–5291 (2020).
53. Kljun, N., Calanca, P., Rotach, M. W. & Schmid, H. P. A simple two-dimensional parameterisation for Flux Footprint Prediction (FFP). *Geosci. Model Dev.* **8**, 3695–3713 (2015).
54. Aubinet, M. et al. Estimates of the annual net carbon and water exchange of forests: the EUROFLUX methodology. *Adv. Ecol. Res.* **30**, 113–175 (2000).
55. Cole, L. E. S., Bhagwat, S. A. & Willis, K. J. Long-term disturbance dynamics and resilience of tropical peat swamp forests. *J. Ecol.* **103**, 16–30 (2015).
56. Hirano, T. et al. Effects of disturbances on the carbon balance of tropical peat swamp forests. *Glob. Change Biol.* **18**, 3410–3422 (2012).
57. Aalde, H. et al. in *2006 IPCC Guidelines for National Greenhouse Gas Inventories* 4.1–4.83 (IPCC, 2006).
58. He, B. et al. Carbon storage and distribution in *Acacia crassicarpa* plantation ecosystem [in Chinese]. *J. Nanjing For. Univ. Nat. Sci.* **33**, 46–50 (2009).
59. Zhang, H., Jiang, Y., Song, M., He, J. & Guan, D. Improving understanding of carbon stock characteristics of *Eucalyptus* and *Acacia* trees in southern China through litter layer and woody debris. *Sci. Rep.* **10**, 4735 (2020). (2020).
60. Mokany, K., Raison, R. & Prokushkin, A. S. Critical analysis of root:shoot ratios in terrestrial biomes. *Glob. Change Biol.* **12**, 84–96 (2006).
61. Manuri, S. et al. Tree biomass equations for tropical peat swamp forest ecosystems in Indonesia. *For. Ecol. Manag.* **334**, 241–253 (2014).
62. Setiawan, B. I., Siregar, S. T., Nawari, Nugroho, A. & Sharma, M. in *15th International PEAT Congress (IPC 2016)* 514–517 (International Peatland Society, 2016).
63. Vickers, D. & Mahrt, L. Quality control and flux sampling problems for tower and aircraft data. *J. Atmos. Ocean. Technol.* **14**, 512–526 (1997).
64. Wilczak, J. M., Oncley, S. P. & Stage, S. A. Sonic anemometer tilt correction algorithms. *Bound.-Layer Meteorol.* **99**, 127–150 (2001).
65. Massman, W. J. A simple method for estimating frequency response corrections for eddy covariance systems. *Agric. For. Meteorol.* **104**, 185–198 (2000).
66. Webb, E. K., Pearman, G. I. & Leuning, R. Correction of flux measurements for density effects due to heat and water vapor transfer. *Q. J. R. Meteorol. Soc.* **106**, 85–100 (1980).
67. Xu, K. E. et al. The eddy-covariance storage term in air: consistent community resources improve flux measurement reliability. *Agric. For. Meteorol.* **279**, 107734 (2019).
68. Foken, T. & Wichura, B. Tools for quality assessment of surface-based flux measurements. *Agric. For. Meteorol.* **78**, 83–105 (1996).
69. Mauder, M. et al. A strategy for quality and uncertainty assessment of long-term eddy-covariance measurements. *Agric. For. Meteorol.* **169**, 122–135 (2013).
70. Papale, D. et al. Towards a standardized processing of net ecosystem exchange measured with eddy covariance technique: algorithms and uncertainty estimation. *Biogeosciences* **3**, 571–583 (2006).
71. Falge, E. et al. Gap-filling strategies for defensible annual sums of net ecosystem exchange. *Agric. For. Meteorol.* **107**, 43–69 (2001).
72. Moffat, A. M. et al. Comprehensive comparison of gap-filling techniques for eddy covariance net carbon fluxes. *Agric. For. Meteorol.* **147**, 209–232 (2007).
73. Papale, D. & Valentini, R. A new assessment of European forests carbon exchanges by eddy fluxes and artificial neural network spatialization. *Glob. Change Biol.* **9**, 525–535 (2003).
74. Xu, T. et al. Evaluating different machine learning methods for upscaling evapotranspiration from flux towers to the regional scale. *J. Geophys. Res. Atmos.* **123**, 8674–8690 (2018).
75. Kim, Y. et al. Gap-filling approaches for eddy covariance methane fluxes: a comparison of three machine learning algorithms and a traditional method with principal component analysis. *Glob. Change Biol.* **26**, 1499–1518 (2020).
76. Kiew, F. et al. CO_2 balance of a secondary tropical peat swamp forest in Sarawak, Malaysia. *Agric. For. Meteorol.* **248**, 494–501 (2018).
77. Wutzler, T. et al. Basic and extensible post-processing of eddy covariance flux data with REddyProc. *Biogeosciences* **15**, 5015–5030 (2018).
78. Reichstein, M. et al. On the separation of net ecosystem exchange into assimilation and ecosystem respiration: review and improved algorithm. *Glob. Change Biol.* **11**, 1424–1439 (2005).
79. Hirano, T., Kusin, K., Limin, S. & Osaki, M. Evapotranspiration of tropical peat swamp forests. *Glob. Change Biol.* **21**, 1914–1927 (2015).
80. Finkelstein, P. L. & Sims, P. F. Sampling error in eddy correlation flux measurements. *J. Geophys. Res.* **106**, 3503–3509 (2001).
81. Deventer, M. J. et al. Error characterization of methane fluxes and budgets derived from a long-term comparison of open- and closed-path eddy covariance systems. *Agric. For. Meteorol.* **278**, 107638 (2019).
82. Griffis, T. J. et al. Hydrometeorological sensitivities of net ecosystem carbon dioxide and methane exchange of an Amazonian palm swamp peatland. *Agric. For. Meteorol.* **295**, 108167 (2020).
83. Wong, G. X. et al. How do land use practices affect methane emissions from tropical peat ecosystems? *Agric. For. Meteorol.* **282–283**, 107869 (2020).
84. Azizan, S. N. F. et al. Comparing GHG emissions from drained oil palm and recovering tropical peatland forests in Malaysia. *Water* **13**, 3372 (2021).
85. Melling, L., Hatano, R. & Goh, K. J. Nitrous oxide emissions from three ecosystems in tropical peatland of Sarawak, Malaysia. *Soil Sci. Plant Nutr.* **53**, 792–805 (2007).

86. Jauhiainen, J. et al. Nitrous oxide fluxes from tropical peat with different disturbance history and management. *Biogeosciences* **9**, 1337–1350 (2012).
87. Inubushi, K., Furukawa, Y., Hadi, A., Purnomo, E. & Tsuruta, H. Seasonal changes of CO_2, CH_4 and N_2O fluxes in relation to land-use change in tropical peatlands located in coastal area of South Kalimantan. *Chemosphere* **52**, 603–608 (2003).
88. Hergoualc'h, K. et al. Spatial and temporal variability of soil N_2O and CH_4 fluxes along a degradation gradient in a palm swamp peat forest in the Peruvian Amazon. *Glob. Change Biol.* **26**, 7198–7216 (2020).
89. Teh, Y. A., Murphy, W. A., Berrio, J., Boom, A. & Page, S. E. Seasonal variability in methane and nitrous oxide fluxes from tropical peatlands in the western Amazon basin. *Biogeosciences* **14**, 3669–3683 (2017).
90. Adji, F. F., Hamada, Y., Darang, U., Limin, S. H. & Hatan, R. Effect of plant-mediated oxygen supply and drainage on greenhouse gas emission from a tropical peatland in Central Kalimantan, Indonesia. *Soil Sci. Plant Nutr.* **60**, 216–230 (2014).

Acknowledgements The establishment and operation of the eddy covariance towers and associated data collection were financed by Asia Pacific Resources International Ltd. (APRIL) and Riau Ecosystem Restoration (RER).

Author contributions C.S.D. conceived the study. C.S.D., A.P.S. and A.R.D. completed eddy covariance data processing. Nardi, A.P.S., Nurholis, M.H., C.S.D., A.R., R.E.M., S.K. and Y.S. collected data and maintained and calibrated the eddy covariance instruments. C.S.D. conceived the paper and wrote the initial draft, to which all authors provided critical contributions and approved submission.

Competing interests C.D.E., S.E.P., S.S., F.A. and D.A. contributed to this paper as part of their role in the Independent Peat Expert Working Group (IPEWG), which was set up by Asia Pacific Resources International Ltd. (APRIL) to provide objective science-based advice on peatland management. The contribution of A.R.D. was also supported by APRIL to provide technical guidance on the eddy covariance data processing, including quality controls and gap-filling protocols. C.S.D., Nardi, A.P.S., Nurholis, M.H., A.R., R.E.M., S.K. and Y.S. are employed by APRIL to conduct field measurements, including eddy covariance instruments maintenance and calibration. The funders had no role in the interpretation of data, in the writing of the manuscript or in the decision to publish the results. The authors declare that all views expressed are their own.

Additional information

Supplementary information The online version contains supplementary material available at https://doi.org/10.1038/s41586-023-05860-9.

Correspondence and requests for materials should be addressed to Chandra S. Deshmukh.

Peer review information *Nature* thanks Daniel Murdiyarso and the other, anonymous, reviewer(s) for their contribution to the peer review of this work. Peer reviewer reports are available.

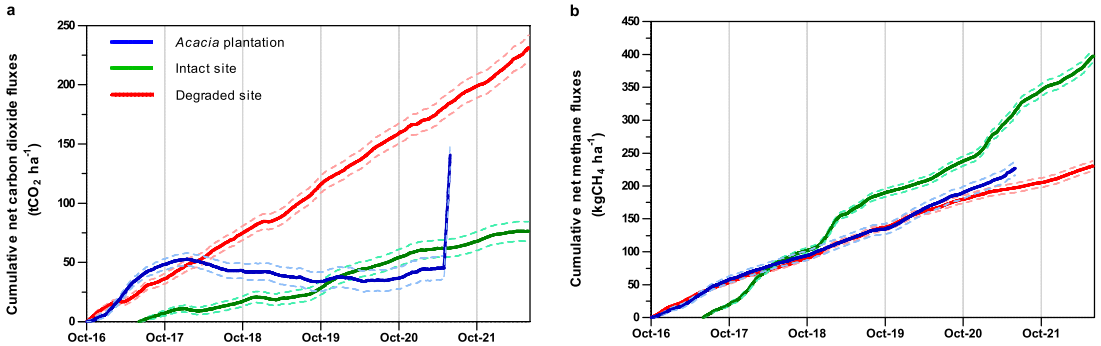

Extended Data Fig. 1 | *Acacia* plantation, degraded and intact peat swamp forest in Sumatra, Indonesia, are emitting CO_2 and CH_4 to the atmosphere. Cumulative measured net CO_2 (**a**) and net CH_4 (**b**) fluxes with cumulative flux uncertainty (random error, friction velocity threshold and gap-filling approach) at the *Acacia* plantation (blue), degraded site (red) and intact site (green). Carbon export in harvested wood at the *Acacia* plantation is added in the end of plantation rotation, conservatively assuming that all harvested C would be returned to the atmosphere as CO_2. Intact and degraded sites were considered to have had no biomass C export during the study period. Positive values indicate emission to the atmosphere.

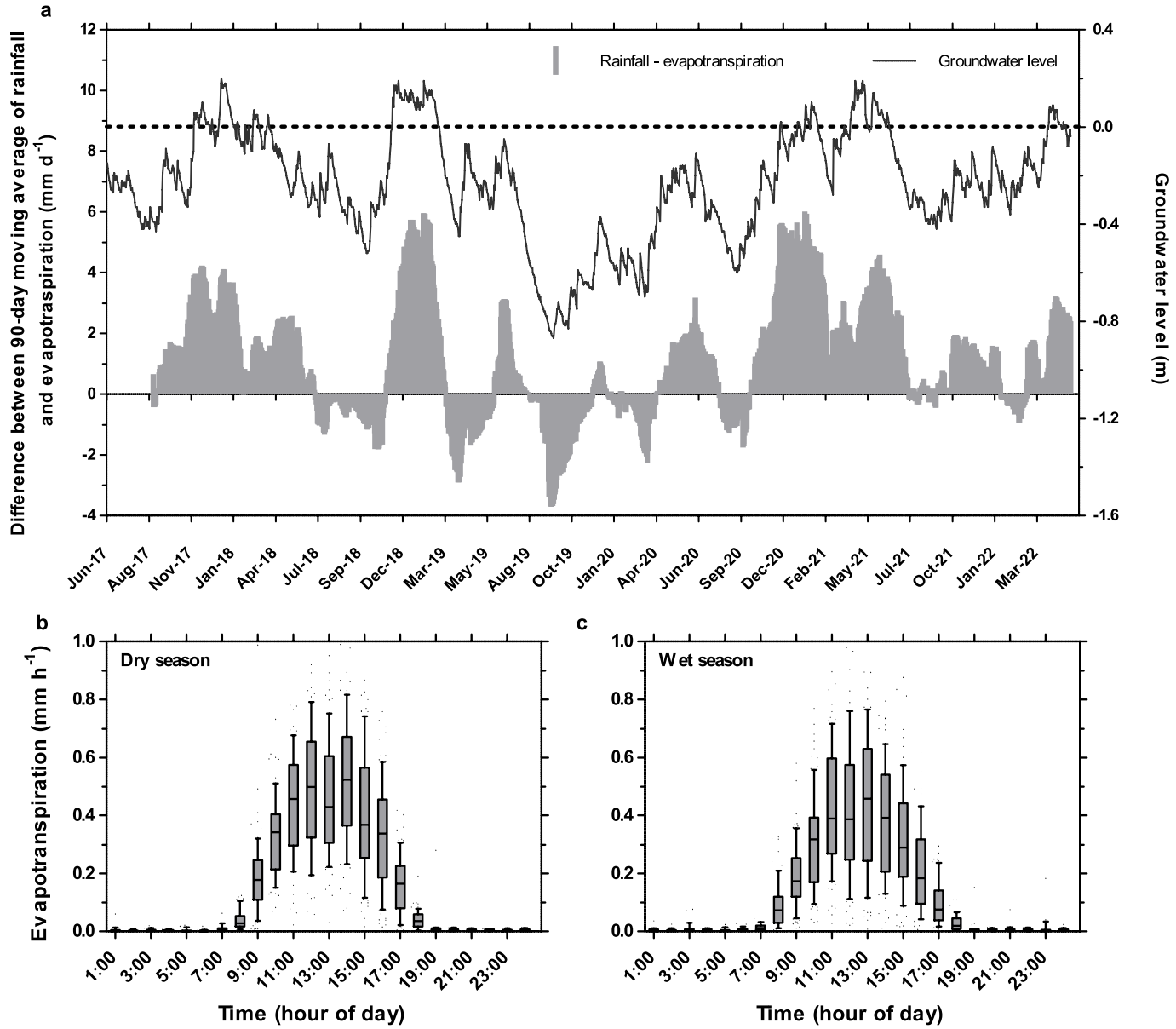

Extended Data Fig. 2 | GWL is controlled by the balance between rainfall and evapotranspiration at intact peat swamp forest in Sumatra, Indonesia. **a**, Time series of average GWL from three piezometers spanning 12 km with difference between 90 days moving average of rainfall and evapotranspiration. Negative difference indicates rainfall deficit. Positive and negative GWL values indicate the water level above and below the peat hollow surface, respectively. Diel pattern of evapotranspiration during dry season (February and July) (**b**) and wet season (April and November) (**c**) over the measurement periods show negligible evapotranspiration in the nighttime. The boxes show the median value and the interquartile range and whiskers denote the full range.

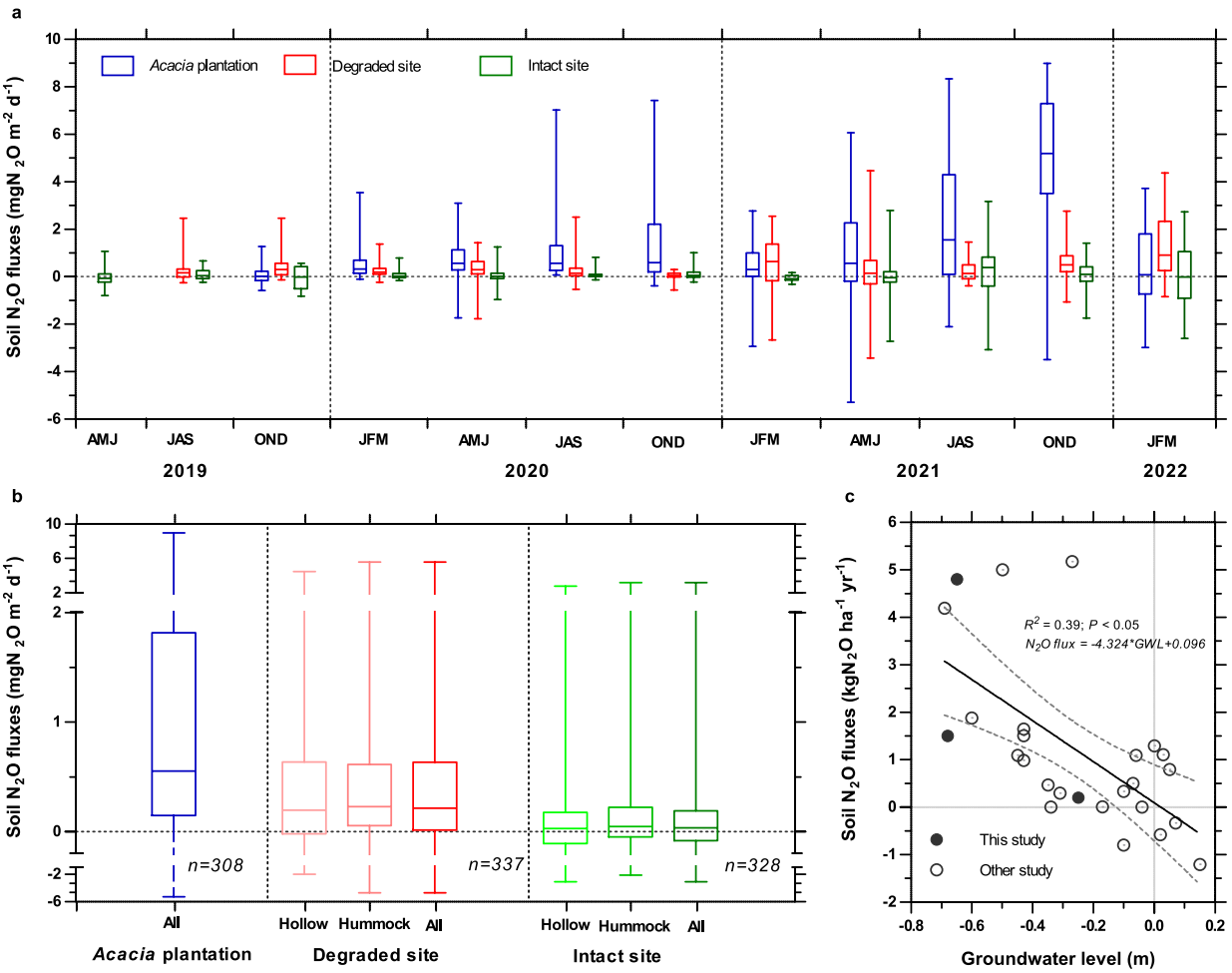

Extended Data Fig. 3 | Soil N_2O emissions increase as GWLs decrease in tropical peatlands. Temporal variation (**a**) and spatial variation (**b**) in soil N_2O fluxes from *Acacia* plantation (blue), degraded site (red) and intact site (green). The boxes show the median value and the interquartile range and whiskers denote the full range of all chambers. The plus signs (+) in the boxes of panel **b** show the average values. The *n* values represent the total number of soil N_2O flux measurements. **c**, Relationship between N_2O fluxes and GWL were derived from soil flux chamber measurements on various land uses across tropical peatlands. Positive and negative GWL values indicate the water level above and below the peat surface, respectively. Positive flux value indicates emission to the atmosphere and negative value indicates uptake by the soil.

Extended Data Table 1 | Characteristics of *Acacia* plantation and degraded and intact peat swamp forest in Sumatra, Indonesia

Parameter	*Acacia* plantation	Degraded peatland	Intact peatland	Method
Tower location	Latitude:0° 30′ 57.221″ N	Latitude: 0° 41′ 58.169″ N	Latitude: 0° 23′ 42.735″ N	
	Longitude: 102° 2′ 11.090″E	Longitude: 102° 47′ 35.898″ E	Longitude: 102° 45′ 52.382″E	
Tower height (m)	40	40	48	
Average canopy height (m)	17 ± 6	19 ± 6	32 ± 6	Permanent sampling plot
Dominant understorey species	*Nephrolepis biserrata, Stenochlaena palustris,* Wild Seedlings of *Acacia crassicarpa*	*Dicranopteris linearis, Nepenthes* spp., *Pandanus* spp., *Cyrtostachys renda, Nephrolepis* sp., *Stenochlaena* sp., *Blechnum* sp.	*Nepenthes* spp., *Pandanus* spp., *Cyrtostachys renda*	Permanent sampling plot
Dominant overstorey species	*Acacia crassicarpa*	*Syzygium claviflorum, Shorea teysmanniana, Stemonurus secundiflorus, Blumeodendron kurzii, Horsfieldia crassifolia, Macaranga pruinosa*	*Shorea uliginosa, Calophyllum ferrugineum, Syzygium* sp., *Camnosperma macrophylla, Tetramerista glabra, Palaquium burckii*	Permanent sampling plot
Surface peat type (0-0.5 m)	Hemic	Fibric	Fibric	Von Post's scale for peat humification
Peat depth (m)	7 ± 0.8	8.4 ± 1.0	9 ± 1.0	Manual peat auger
Peat bulk density (g cm^{-3}) (0-0.5 m)	0.20 ± 0.06	0.09 ± 0.03	0.08 ± 0.03	Gravimetric
Peat pH (0-0.5 m)	3.4 ± 0.1	3.6 ± 0.3	3.6 ± 0.1	pH 1:5
Peat ash content (%)(0-0.5 m)	2.5 ± 1.2	1.5 ± 0.9	0.8 ± 0.5	Loss on ignition
Peat carbon concentration (%) (0-0.5 m)	54.5 ± 1.0	57.3 ± 0.1	55.9 ± 0.7	Combustion
Peat nitrogen concentration (%) (0-0.5 m)	1.4 ± 0.10	1.5 ± 0.10	1.6 ± 0.10	
Peat nitrate concentration (ppm) (0-0.5 m)	2,072 ± 610	1,588 ± 725	1,167 ± 509	Titration
Peat ammonium concentration (ppm) (0-0.5 m)	680 ± 85	654 ± 184	475 ± 130	

Values represent averages with standard deviation.

Extended Data Table 2 | Annual average with standard deviation of environmental variables at *Acacia* plantation and degraded and intact peat swamp forest in Sumatra, Indonesia

Measurement period	Average air temperature (°C)	Average soil temperature (°C)	Average soil water temperature (°C)	Annual rainfall (mm yr^{-1})	Number of day without rain	Annual evapotranspiration (mm yr^{-1})	Number of day with daily rainfall < daily evapotranspiration (%)	Groundwater level (m)
***Acacia* plantation**								
October 2016 - September 2017	27.2 ± 1.0	30.2 ± 1.1	29.3 ± 0.4	2,687	223	1,465	251 (69%)	-0.66 ± 0.16
October 2017 - September 2018	26.9 ± 0.9	28.8 ± 0.7	28.6 ± 0.2	1,651	260	1,527	283 (78%)	-0.68 ± 0.07
October 2018 - September 2019	27.0 ± 0.8	28.9 ± 0.7	28.2 ± 0.5	2,177	238	1,597	259 (71%)	-0.67 ± 0.18
October 2019 - September 2020	27.0 ± 1.2	29.4 ± 0.5	28.7 ± 0.2	2,232	251	1,635	275 (75%)	-0.59 ± 0.23
October 2020 - May 2021	26.6 ± 1.2	29.4 ± 0.8	28.4 ± 0.3	1,655*	145*	843*	173* (71%)	-0.69 ± 0.16
October 2016 - May 2021	27.0 ± 1.0	29.3 ± 1.0	28.7 ± 0.5	2,228		1,514		-0.65 ± 0.17
Degraded site								
October 2016 - September 2017	26.8 ± 0.9		28.4 ± 0.3	2,142	243	1,372	277 (76%)	-0.51 ± 0.13
October 2017 - September 2018	26.7 ± 0.9		27.7 ± 0.2	1,837	232	1,371	280 (77%)	-0.67 ± 0.10
October 2018 - September 2019	27.2 ± 0.9		27.2 ± 0.1	1,325	264	1,539	297 (81%)	-0.79 ± 0.21
October 2019 - September 2020	28.1 ± 1.3		27.5 ± 0.1	1,763	240	1,496	283 (78%)	-0.73 ± 0.14
October 2020 - September 2021	28.2 ± 1.0		27.8 ± 0.3	2,206	230	1,351	265 (73%)	-0.70 ± 0.17
October 2021 - May 2022	28.5 ± 1.0		27.8 ± 0.2	1,347*	151*	869*	176* (72%)	-0.72 ± 0.13
October 2016 - May 2022	27.5 ± 1.2		27.7 ± 0.3	1,942		1,411		-0.69 ± 0.18
Intact site								
June 2017 - May 2018	26.6 ± 0.9	27.2 ± 0.5	26.2 ± 0.2	2,020	226	1,537	271 (74%)	-0.15 ± 0.16
June 2018 - May 2019	26.9 ± 0.9	27.4 ± 0.1	25.7 ± 0.1	1,756	240	1,592	288 (79%)	-0.21 ± 0.20
June 2019 - May 2020	27.0 ± 0.9	28.1 ± 0.1	25.7 ± 0.1	1,496	246	1,547	289 (79%)	-0.47 ± 0.18
June 2020 - May 2021	26.9 ± 1.1	27.4 ± 0.6	25.7 ± 0.2	2,249	220	1,502	269 (74%)	-0.17 ± 0.20
June 2021 - May 2022	27.3 ± 0.8	27.3 ± 0.2	25.4 ± 0.1	1,895	220	1,471	276 (76%)	-0.19 ± 0.13
June 2017 - May 2022	26.9 ± 1.0	27.5 ± 0.5	25.7 ± 0.2	1,883		1,530		-0.24 ± 0.22

GWLs were averaged from 11 locations around the *Acacia* plantation tower site, four locations around the degraded tower site and 15 locations in the intact site. The numbers marked with an asterisk (*) are cumulative estimates over eight months. Negative GWL values indicate the water level below the peat hollow surface.

Extended Data Table 3 | Net ecosystem CO_2 and CH_4 exchanges measured using eddy covariance over *Acacia* plantation and degraded and intact peat swamp forest in Sumatra, Indonesia

Measurement Period	Annual net ecosystem CO_2 exchange ($tCO_2\ ha^{-1}\ yr^{-1}$)	Annual net ecosystem CH_4 exchange ($kgCH_4\ ha^{-1}\ yr^{-1}$)	Annual oxidative peat decomposition ($tCO_2\ ha^{-1}\ yr^{-1}$)
***Acacia* plantation**			
October 2016 - September 2017	48.4 ± 4.7	57.9 ± 5.1	41.2 ± 8.9
October 2017 - September 2018	-5.4 ± 4.7	36.4 ± 5.0	38.4 ± 8.4
October 2018 - September 2019	-8.8 ± 4.5	40.4 ± 3.8	45.3 ± 9.2
October 2019 - September 2020	2.7 ± 4.4	55.3 ± 4.3	41.8 ± 9.9
October 2020 - May 2021	11.7 ± 6.0	37.1 ± 5.0	42.4 ± 9.5
October 2016 - May 2021	9.5 ± 4.5	48.6 ± 4.1	41.7 ± 9.5
Degraded site			
October 2016 - September 2017	36.3 ± 4.2	53.3 ± 2.4	
October 2017 - September 2018	38.7 ± 4.1	37.3 ± 2.2	
October 2018 - September 2019	40.9 ± 4.1	46.5 ± 3.6	
October 2019 - September 2020	43.1 ± 4.4	42.6 ± 3.3	
October 2020 - September 2021	39.9 ± 5.2	25.4 ± 4.3	
October 2021 - May 2022	48.8 ± 5.4	25.3 ± 2.9	
October 2016 - May 2022	40.8 ± 4.4	40.7 ± 3.2	
Intact site			
June 2017 - May 2018	11.9 ± 3.7	86.7 ± 3.9	
June 2018 - May 2019	9.1 ± 3.7	83.0 ± 3.6	
June 2019 - May 2020	25.6 ± 4.1	46.6 ± 4.5	
June 2020 - May 2021	15.8 ± 3.5	97.3 ± 5.4	
June 2021 - May 2022	14.0 ± 3.4	84.0 ± 4.3	
June 2017 - May 2022	15.3 ± 3.7	79.5 ± 4.4	

Annual estimates with total uncertainty includes random error, friction velocity criteria and gap-filling approach. Annual oxidative peat decomposition measured using the soil-chamber technique at the *Acacia* plantation is given with standard deviation from four soil flux chambers. Positive values indicate emission to the atmosphere, negative values indicate net uptake by the ecosystem.

Extended Data Table 4 | GHG balance of *Acacia* plantation and degraded and intact peat swamp forest in Sumatra, Indonesia

Parameter	Intact site	Degraded site	*Acacia* plantation
Net ecosystem CO_2 exchange (tCO_2 ha^{-1} yr^{-1})[a]	15.3 ± 3.7	40.8 ± 4.4	9.5 ± 4.5
C-export in harvested wood (tCO_2 ha^{-1} yr^{-1})[b]			20.5 ± 1.1
Fluvial C-export (tC ha^{-1} yr^{-1})[b]	0.3 ± 0.1	0.5 ± 0.1	0.4 ± 0.1
Net ecosystem CH_4 exchange (kg CH_4 ha^{-1} yr^{-1})[a]	79.5 ± 4.4	40.7 ± 3.2	48.6 ± 4.1
Soil N_2O flux (kg N_2O ha^{-1} yr^{-1})[b]	0.3 ± 0.5	2.2 ± 2.3	4.8 ± 3.8
GHG balance (tCO_2-eq ha^{-1} yr^{-1})			
Net ecosystem CO_2 exchange	15.3 ± 3.7	40.8 ± 4.4	9.5 ± 4.5
C-export in harvested wood			20.5 ± 1.1
Fluvial C-export	1.1 ± 0.2	1.8 ± 0.4	1.6 ± 0.4
Net ecosystem CH_4 exchange	3.6 ± 0.2	1.8 ± 0.1	2.2 ± 0.2
Soil N_2O flux	0.1 ± 0.1	0.6 ± 0.6	1.3 ± 1.0
Total[c]	20.3 ± 3.7	45.1 ± 4.4	35.2 ± 4.7
Biomass C-loss due to land-use change (tCO_2-eq ha^{-1} yr^{-1})[b]		0.9 ± 0.0	[d]2.4 ± 0.9 to 3.2 ± 0.9
Net impact of land-use change from intact site (tCO_2-eq ha^{-1} yr^{-1})[c]		**25.7 ± 5.7**	**18.1 ± 6.0**
Net impact of land-use change from degraded site (tCO_2-eq ha^{-1} yr^{-1})[c]			**-7.5 ± 6.5**
Avoided emission from bioenergy production (tCO_2-eq ha^{-1} yr^{-1})[b]			-7.3 ± 0.4

To quantify total GHG balance in CO_2 equivalent (CO_2-eq), we used a sustained-flux global-warming potential (SGWP) of 1, 45 and 270 for CO_2, CH_4 and N_2O, respectively, over a 100-year time period[39]. Total GHG balance = (net ecosystem CO_2 exchange + net ecosystem CH_4-C exchange + fluvial C export + C export in harvested wood, where applicable) + (net ecosystem CH_4 exchange × SGWP) + (soil N_2O flux × SGWP). We assumed that all fluvial C export is ultimately converted to CO_2 (ref. 38). Avoided emissions from bioenergy production is calculated by assuming that 54% of harvested wood is used for bioenergy production (details in Supplementary Method 4). [a]Values represent average with total uncertainty from random error, friction velocity threshold and gap-filling approach. [b]Values represent average with standard deviation. [c]Values represent total with standard deviation calculated from propagation of errors. [d]Lower and upper ranges represent biomass C loss owing to establishment of *Acacia* plantation on the degraded and intact sites, respectively. The bold numbers indicate net impact of land-use change. Positive value indicates emission to the atmosphere and negative value indicates avoided emission.

Extended Data Table 5 | Average and standard deviation of peat subsidence at *Acacia* plantation and degraded and intact peat swamp forest in Sumatra, Indonesia

	Measurement period	Total subsidence (cm)	Annual subsidence rate (cm yr^{-1})	Groundwater level (m)
Acacia plantation	Full period (October 2016 - May 2021)	-12.1 ± 3.7	-3.0 ± 0.9	-0.65 ± 0.17
	El Niño/IOD-linked drought event (January 2019 - December 2019)	-7.1 ± 2.4	-7.1 ± 2.4	-0.74 ± 0.19
Degraded site	Full period (December 2017 - May 2022)	-16.0 ± 6.0	-3.6 ± 1.2	-0.69 ± 0.18
	El Niño/IOD-linked drought event (January 2019 - December 2019)	-6.9 ± 3.8	-6.9 ± 3.8	-0.74 ± 0.12
Intact site (3 to 6 km from plantation boundary)	Full period (December 2017 - May 2022)	-7.1 ± 2.4	-1.4 ± 1.6	-0.24 ± 0.22
	El Niño/IOD-linked drought event (January 2019 - December 2019)	-7.0 ± 1.3	-7.0 ± 1.6	-0.42 ± 0.11
Intact site (7 to 10 km from plantation boundary)	Full period (December 2017 - May 2022)	-7.0 ± 1.6	-1.4 ± 1.5	-0.24 ± 0.07
	El Niño/IOD-linked drought event (January 2019 - December 2019)	-7.2 ± 1.1	-7.2 ± 1.1	-0.40 ± 0.07

Subsidence rates are strongly affected by the El Niño/IOD-linked drought event in 2019. Peat subsidence rates were derived from 11 locations in the *Acacia* plantation, four locations in the degraded site and 14 locations in the intact site (see Methods). Negative peat subsidence values indicate that the ground surface was falling. Negative GWL values indicate the water level below the peat hollow surface.

Extended Data Table 6 | Land use and locations of tropical peatland sites used in net ecosystem exchanges of CO_2 and CH_4 and soil N_2O syntheses

Land-use	Location	Groundwater level (m)	Flux	Reference
Net carbon dioxide flux (tCO_2 ha^{-1} yr^{-1})				
Secondary forest	Sebangau peat swamp forest, Central Kalimantan, Indonesia	-0.19	-4.9	56
Undrained forest	Block C of mega rice project, Central Kalimantan, Indonesia	-0.14	6.4	56
Drained forest	Betong peat swamp forest, Sarawak, Malaysia	-0.55	14.1	76
Palm swamp forest	Quistococha forest reserve, Loreto, Peru	0.03	-17.0	82
Intact site	Kampar Peninsula, Riau, Indonesia	-0.25	15.3	This study,17
Degraded site	Kampar Peninsula, Riau, Indonesia	-0.68	40.8	This study,17
Acacia plantation	Kampar Peninsula, Riau, Indonesia	-0.65	30.0	This study
Net ecosystem methane exchange (tCH_4 ha^{-1} yr^{-1})				
Undrained forest	Alan Batu forest of Maludam Peninsula, Sarawak, Malaysia	-0.05	0.11	28
Drained forest	Border of Alan Bunga and Batang Alan forest of Maludam Peninsula, Sarawak, Malaysia	-0.19	0.06	28
Oil palm	Sibu, Sarawak, Malaysia	-0.62	0.03	28
Peat swamp forest	Quistococha forest reserve, Loreto, Peru	0.03	0.29	82
Intact site	Kampar Peninsula, Riau, Indonesia	-0.25	0.08	This study,17
Degraded site	Kampar Peninsula, Riau, Indonesia	-0.68	0.04	This study,17
Acacia plantation	Kampar Peninsula, Riau, Indonesia	-0.65	0.05	This study
Soil nitrous oxide flux (kgN_2O ha^{-1} yr^{-1})				
Oil palm	Raja Musa peat swamp forest reserve, Selangor, Malaysia	-0.69	4.20	83
Natural forest	Raja Musa peat swamp forest reserve, Selangor, Malaysia	0.05	0.80	83
Natural forest	Mukah devision, Serawak, Malaysia	-0.45	1.10	84
Sago	Mukah devision, Serawak, Malaysia	-0.27	5.18	84
Oil palm	Mukah devision, Serawak, Malaysia	-0.60	1.88	84
Undrained forest	Sebangau peat swamp forest, Central Kalimantan, Indonesia	-0.10	0.34	85
Drained recovering forest	Block C of mega rice project, Central Kalimantan, Indonesia	-0.31	0.30	85
Drained burned peat	Block C of mega rice project, Central Kalimantan, Indonesia	-0.43	1.51	85
Agricultural peat	Kalampangan, Central Kalimantan, Indonesia	-0.43	1.65	85
Agricultural peat	Marang, Central Kalimantan, Indonesia	-0.43	0.99	85
Abandoned paddy fields	South Kalimantan, Indonesia	0.02	-0.58	86
Secondary forest	South Kalimantan, Indonesia	-0.10	-0.80	86
Intact peatland	Northern Peruvian Amazon, Loreto, Peru	0.00	1.30	87
Medium degraded	Northern Peruvian Amazon, Loreto, Peru	-0.07	0.50	87
High degraded	Northern Peruvian Amazon, Loreto, Peru	-0.06	1.10	87
Forested vegetation	Pastaza-Marañón foreland basin, Peru	-0.34	0.00	88
Palm swamp	Pastaza-Marañón foreland basin, Peru	-0.17	0.01	88
Forested pole	Pastaza-Marañón foreland basin, Peru	-0.04	0.00	88
Flooded forest	Sebangau peat swamp forest, Central Kalimantan, Indonesia	0.07	-0.33	89
Drained forest	Block C of mega rice project, Central Kalimantan, Indonesia	-0.35	0.47	89
Burnt flooded plain	Sebangau peat swamp forest, Central Kalimantan, Indonesia	0.15	-1.20	89
Drained burnt	Block C of mega rice project, Central Kalimantan, Indonesia	0.03	1.11	89
Oil palm	Pangkalan Bun, Central Kalimantan, Indonesia	-0.50	5	24
Intact site	Kampar Peninsula, Riau, Indonesia	-0.25	0.3	This study,17
Degraded site	Kampar Peninsula, Riau, Indonesia	-0.68	2.2	This study,17
Acacia plantation	Kampar Peninsula, Riau, Indonesia	-0.65	4.8	This study

Positive and negative GWL values indicate the water level above and below the peat hollow surface, respectively. Positive flux value indicates emission to the atmosphere and negative value indicates uptake by the ecosystem. References[82-90].

nature portfolio

Corresponding author(s): Chandra Shekhar Deshmukh

Last updated by author(s): Jan 3, 2023

Reporting Summary

Nature Portfolio wishes to improve the reproducibility of the work that we publish. This form provides structure for consistency and transparency in reporting. For further information on Nature Portfolio policies, see our Editorial Policies and the Editorial Policy Checklist.

Statistics

For all statistical analyses, confirm that the following items are present in the figure legend, table legend, main text, or Methods section.

n/a	Confirmed
☐	☒ The exact sample size (*n*) for each experimental group/condition, given as a discrete number and unit of measurement
☐	☒ A statement on whether measurements were taken from distinct samples or whether the same sample was measured repeatedly
☐	☒ The statistical test(s) used AND whether they are one- or two-sided *Only common tests should be described solely by name; describe more complex techniques in the Methods section.*
☒	☐ A description of all covariates tested
☐	☒ A description of any assumptions or corrections, such as tests of normality and adjustment for multiple comparisons
☐	☒ A full description of the statistical parameters including central tendency (e.g. means) or other basic estimates (e.g. regression coefficient) AND variation (e.g. standard deviation) or associated estimates of uncertainty (e.g. confidence intervals)
☐	☒ For null hypothesis testing, the test statistic (e.g. *F*, *t*, *r*) with confidence intervals, effect sizes, degrees of freedom and *P* value noted *Give P values as exact values whenever suitable.*
☒	☐ For Bayesian analysis, information on the choice of priors and Markov chain Monte Carlo settings
☒	☐ For hierarchical and complex designs, identification of the appropriate level for tests and full reporting of outcomes
☒	☐ Estimates of effect sizes (e.g. Cohen's *d*, Pearson's *r*), indicating how they were calculated

Our web collection on statistics for biologists contains articles on many of the points above.

Software and code

Policy information about availability of computer code

Data collection	LI-7200RS commercial software (version 8.0.0, LI-COR) for downloading eddy covariance raw data; LI-8100A commercial software (version 4.0.0, LI-COR) for downloading CO2 concentration profiles and oxidative peat decomposition data; LoggerSW commercial software (version 4.0, Sollinst) for downloading the groundwater level data.
Data analysis	EddyPro commercial software (version 6.2.0, LI-COR) for preliminary CO2, CH4 and H2O eddy covariance data processing; SoilFluxPro commercial software (version 4.0, LI-COR) for preliminary oxidative peat decomposition and storage term data processing.

For manuscripts utilizing custom algorithms or software that are central to the research but not yet described in published literature, software must be made available to editors and reviewers. We strongly encourage code deposition in a community repository (e.g. GitHub). See the Nature Portfolio guidelines for submitting code & software for further information.

Data

Policy information about availability of data

All manuscripts must include a data availability statement. This statement should provide the following information, where applicable:

- Accession codes, unique identifiers, or web links for publicly available datasets
- A description of any restrictions on data availability
- For clinical datasets or third party data, please ensure that the statement adheres to our policy

All data that support the findings of this study are archived on https://doi.org/10.5281/zenodo.7500659

Human research participants

Policy information about studies involving human research participants and Sex and Gender in Research.

Reporting on sex and gender	*Use the terms sex (biological attribute) and gender (shaped by social and cultural circumstances) carefully in order to avoid confusing both terms. Indicate if findings apply to only one sex or gender; describe whether sex and gender were considered in study design whether sex and/or gender was determined based on self-reporting or assigned and methods used. Provide in the source data disaggregated sex and gender data where this information has been collected, and consent has been obtained for sharing of individual-level data; provide overall numbers in this Reporting Summary. Please state if this information has not been collected. Report sex- and gender-based analyses where performed, justify reasons for lack of sex- and gender-based analysis.*
Population characteristics	*Describe the covariate-relevant population characteristics of the human research participants (e.g. age, genotypic information, past and current diagnosis and treatment categories). If you filled out the behavioural & social sciences study design questions and have nothing to add here, write "See above."*
Recruitment	*Describe how participants were recruited. Outline any potential self-selection bias or other biases that may be present and how these are likely to impact results.*
Ethics oversight	*Identify the organization(s) that approved the study protocol.*

Note that full information on the approval of the study protocol must also be provided in the manuscript.

Field-specific reporting

Please select the one below that is the best fit for your research. If you are not sure, read the appropriate sections before making your selection.

☐ Life sciences ☐ Behavioural & social sciences ☒ Ecological, evolutionary & environmental sciences

For a reference copy of the document with all sections, see nature.com/documents/nr-reporting-summary-flat.pdf

Ecological, evolutionary & environmental sciences study design

All studies must disclose on these points even when the disclosure is negative.

Study description	The study reports net ecosystem exchanges of carbon dioxide (CO2) and methane (CH4) as well as soil nitrous oxide (N2O) fluxes from Acacia crassicarpa plantation, degraded site and intact site within the same peat landscape to represent land-cover change trajectories in Sumatra, Indonesia. The study reports the first full plantation rotation GHG balance investigation undertaken in any fiber wood plantation on peatland globally. The GHG emissions from the Acacia plantation over a full plantation rotation were two times higher than those from the intact site, but only around half of the current IPCC Tier 1 emission factor for this land-use. Our results should help to reduce the uncertainty in the estimation of GHG emissions from globally important ecosystems, provide estimate of the impact of land-use change on tropical peat, and develop science-based peatland management practices as nature-based climate solutions that help to minimize GHG emissions.
Research sample	We quantified all major GHG flux terms (net ecosystem exchanges of CO2 and CH4, and soil N2O flux), including fluvial C-exports for Acacia crassicarpa plantation, degraded and intact sites within the same peat landscape in Sumatra, Indonesia. In addition, biomass C-loss due to plantation establishment and C-export in harvested wood for Acacia plantation were also quantified. The peat chemical and physical properties, groundwater level, and meteorological variables at all sites were measured.
Sampling strategy	We quantified GHG balance of fiber wood plantation on tropical peatland in Sumatra, Indonesia to cover a full plantation rotation (planting - plantation growth - harvesting) and all major GHG flux terms (net ecosystem exchanges of CO2 and CH4, and soil N2O flux), including biomass C-loss due to plantation establishment, C-export in harvested wood and fluvial C-exports. We compared the GHG balance at the fiber wood plantation with more than five years of measurements at the degraded and five years of measurements at the intact sites on the same peat landscape.
Data collection	Measurements of net ecosystem CO2 and CH4 exchanges were conducted using eddy covariance technique. Eddy covariance system consisted of an enclosed-path CO2/H2O analyzer (LI-7200, LI-COR) to measure CO2 and H2O concentrations, an open path CH4 analyzer (LI-7700, LI-COR) to measure CH4 concentrations, and a three-dimensional sonic anemometer (WindMaster Pro3-Axis Anemometer, Gill Instruments) to measure the orthogonal components of wind-speed fluctuations at 40, 40, and 48 m heights above ground surface for Acacia plantation, degraded, and intact sites, respectively. Soil N2O flux was measured using manual flux chamber technique, following gas chromatograph analysis. Peat oxidative decomposition was measured using automated chamber system (LI-8100-104, LI-COR) consisting of white enamel-coated stainless steel chambers connected to soil CO2 analyzer (LI-8100, LI-COR). For peat physical and chemical properties of the surface layer (0 - 50 cm) , four plots in each of the Acacia plantation and degraded site, and three plots in the intact site were randomly selected within the eddy covariance flux footprint (200 - 1,000 m distance from each tower location).
Timing and spatial scale	We collected continuous eddy covariance measurements over the full Acacia plantation cycle (planting - plantation growth - harvesting, October 2016 to May 2021), the degraded site (October 2016 to May 2022) and the intact site (June 2017 to May 2022). The raw eddy covariance data were recorded at 10 Hz frequency and fluxes were calculated at every 30 minutes. The eddy

covariance measurements represent an area within 1,000 m radius from the eddy covariance tower.
Soil N2O fluxes measurements were made between December 2019 and March 2022 for the plantation site, between July 2019 and March 2022 for the degraded site, and between June 2019 and February 2022 for the intact site on a bi-monthly basis. Four plots in each of the Acacia plantation and degraded site, and three plots in the intact within eddy covariance flux footprint (200 - 1,000 m distance from the eddy covariance tower location). At each plot in the degraded and intact sites, two stainless steel rectangular collars on hummocks and four in the adjacent hollows, whereas four collars per plot in the plantation (around 50-100 m apart) were inserted permanently 15 cm into the peat five months before the start of the flux monitoring.
Peat oxidative decomposition collected continuously in between October 2016 to May 2021 at 30 minutes frequency with four replicates.
For peat physical and chemical properties of the surface layer (0 - 50 cm), four plots in each of the Acacia plantation and degraded site, and three plots in the intact site within the eddy covariance flux footprint (200 - 1,000 m distance from each tower location). Peat samples for bulk density, pH and ash content were collected in September 2017, February 2019 and September 2019 in the intact site, in June 2017, January 2018, October 2018, and February 2019 in the degraded site and June 2017, February 2018, October 2018, February 2019 and October 2019 in the Acacia plantation. Samples for soil carbon, nitrogen, nitrate, ammonium content were collected in August 2020 and October 2021 for all sites.

Data exclusions

Following standard eddy covariance quality control criteria, we applied quality controls to remove low-quality eddy covariance measurements, as is done for eddy covariance measurements (details are in the manuscript). We removed oxidative peat decomposition measurements with negative values, fluxes with coefficients of regression of < 0.9, or values that were extreme outliers (≥ 99th percentile).

Reproducibility

Not applicable due to the nature of the research

Randomization

Sampling plots and collars for soil N2O fluxes monitoring and plots for peat soil sampling were located randomly around each eddy covariance tower within flux footprint i.e. 200 - 1000 m radius from eddy covariance tower.

Blinding

Not applicable due to the nature of the research

Did the study involve field work? ☒ Yes ☐ No

Field work, collection and transport

Field conditions

This study was conducted in the Kampar Peninsula (Sumatra, Indonesia), an ombrogenous tropical peatland of around 700,000 ha that largely formed within the past 5,100 years. The base of the peatland is grey marine clays over which peat varies from approximately 3 m deep near the river boundaries, to over 11 m in the center of the approximately 60-km-wide and > 100-km-long peat dome, with an average depth of 8 m. The peninsula experiences a humid tropical climate with the average monthly air temperature ranging from 26 to 29 °C. The variability in rainfall is influenced by monsoonal processes combined with El Niño-Southern Oscillation (ENSO) and Indian Ocean Dipole (IOD). In general, the El Niño and positive IOD occur sequentially, with the positive IOD peaking a few months after the El Niño, exerting a strong combined effect on regional rainfall patterns. The average annual rainfall for the past eight years (2014-2021, with El Niño in 2015, La Niña in 2017 and a major positive IOD combined with an El Niño event in 2019) is 1,772 ± 201 mm. Rainfall varies seasonally with two annual peaks, in November-December and another in March-April.

Location

Acacia plantation. Latitude : 0° 30′ 57.221″ N; Longitude : 102° 2′ 11.090″E; vegetation-canopy height : 17 ± 6 m; peat depth : 7 ± 0.8 m; groundwater level : -0.65 ± 0.17 m.
Degraded peat swamp forest. Latitude : 0° 41′ 58.169″ N; Longitude : 102° 47′ 35.898″ E; vegetation-canopy height: 19 ± 6 m; peat depth : 8.4 ± 1.0 m; groundwater level : -0.69 ± 0.18 m.
Intact peat swamp forest. Latitude : 0° 23′ 42.735″ N; Longitude: 102° 45′ 52.382″E; vegetation-canopy height : 32 ± 6 m; peat depth : 9 ± 1.0 m; groundwater level : -0.24 ± 0.22 m.

Access & import/export

No sample import/export efforts have been made in this study. The establishment and operation of the eddy covariance towers and associated data collection were funded and approved by Asia Pacific Resources International Ltd (APRIL) and Riau Ecosystem Restoration (RER). Acacia plantation site is managed by APRIL, the degraded site was an unmanaged area which located in the Acacia plantation boundary, whereas the intact site is located in the RER conservation area.

Disturbance

No disturbance has been caused due to this study.

Reporting for specific materials, systems and methods

We require information from authors about some types of materials, experimental systems and methods used in many studies. Here, indicate whether each material, system or method listed is relevant to your study. If you are not sure if a list item applies to your research, read the appropriate section before selecting a response.

Materials & experimental systems

n/a	Involved in the study
☒	☐ Antibodies
☒	☐ Eukaryotic cell lines
☒	☐ Palaeontology and archaeology
☒	☐ Animals and other organisms
☒	☐ Clinical data
☒	☐ Dual use research of concern

Methods

n/a	Involved in the study
☒	☐ ChIP-seq
☒	☐ Flow cytometry
☒	☐ MRI-based neuroimaging